



## **Annual phytoplankton succession results from niche-environment interaction**

Mariarita Caracciolo, Gregory Beaugrand, Pierre Hélaouët, Francois Gevaert,  
Martin Edwards, Fabrice Lizon, Loïck Kléparski, Eric Goberville

### **► To cite this version:**

Mariarita Caracciolo, Gregory Beaugrand, Pierre Hélaouët, Francois Gevaert, Martin Edwards, et al..  
Annual phytoplankton succession results from niche-environment interaction. *Journal of Plankton  
Research*, 2021, 43 (1), pp.85-102. 10.1093/plankt/fbaa060 . hal-03267611

**HAL Id: hal-03267611**

**<https://hal.sorbonne-universite.fr/hal-03267611>**

Submitted on 22 Jun 2021

**HAL** is a multi-disciplinary open access archive for the deposit and dissemination of scientific research documents, whether they are published or not. The documents may come from teaching and research institutions in France or abroad, or from public or private research centers.

L'archive ouverte pluridisciplinaire **HAL**, est destinée au dépôt et à la diffusion de documents scientifiques de niveau recherche, publiés ou non, émanant des établissements d'enseignement et de recherche français ou étrangers, des laboratoires publics ou privés.

# Annual phytoplankton succession results from niche-environment interaction

Mariarita Caracciolo<sup>1</sup>, Grégory Beaugrand<sup>2,3,4</sup>, Pierre Helaouët<sup>4</sup>, François Gevaert<sup>3</sup>, Martin Edwards<sup>4,5</sup>, Fabrice Lizon<sup>3</sup>, Loïck Kléparski<sup>2,3,4</sup>, Eric Goberville<sup>6</sup>.

<sup>1</sup>*Sorbonne Université, CNRS, Station Biologique de Roscoff, UMR 7144, ECOMAP, Place Georges Teissier, 29680 Roscoff, France.*

<sup>2</sup>*Centre National de la Recherche Scientifique (CNRS), Université de Lille, Université Littoral Côte d'Opale, UMR 8187, LOG, Laboratoire d'Océanologie et de Géosciences, F 62930 Wimereux, France.*

<sup>3</sup>*Université de Lille, CNRS, Univ. Littoral Côte d'Opale, UMR 8187, LOG, Laboratoire d'Océanologie et de Géosciences, F 62930 Wimereux, France.*

<sup>4</sup>*Marine Biological Association, Citadel Hill, Plymouth PL1 2PB, UK.*

<sup>5</sup>*University of Plymouth, School of Biological and Marine Sciences, Drake Circus, Plymouth, UK.*

<sup>6</sup>*Unité Biologie des organismes et écosystèmes aquatiques (BOREA), Muséum National d'Histoire Naturelle, Sorbonne Université, Université de Caen Normandie, Université des Antilles, CNRS, IRD, CP53, 61, Rue Buffon 75005 Paris, France.*

**Corresponding authors:** Mariarita Caracciolo ([mariarita.caracciolo@sb-roscoff.fr](mailto:mariarita.caracciolo@sb-roscoff.fr)) and Gregory Beaugrand ([Gregory.Beaugrand@univ-lille.fr](mailto:Gregory.Beaugrand@univ-lille.fr))

## **Abstract**

Annual plankton succession has been investigated for many decades and hypotheses ranging from abiotic to biotic mechanisms have been proposed to explain this recurrent pattern. Here, using data collected by the Continuous Plankton Recorder (CPR) survey and models originating from the MacroEcological Theory on the Arrangement of Life (METAL), we investigate annual phytoplankton succession in the North Sea at a species level. Our results show that this phenomenon can be well predicted by models combining photosynthetically active radiation, temperature and macro-nutrients. Our findings suggest that annual phytoplankton succession, at community level, originates from the interaction between species ecological niche and annual environmental fluctuations. We discuss our results in the context of traditional hypotheses formulated to explain this recurrent pattern in the marine field, including those on the initiation, the development and the termination of a typical extratropical spring bloom.

## **Keywords**

Annual plankton succession, phenology, ecological niche, environment, plankton, Continuous Plankton Recorder (CPR), METAL theory.

## 1. INTRODUCTION

Annual Plankton Succession (APS) is defined as the recurrent pattern of species abundance observed during the annual cycle (Cushing 1959, Winder and Cloern 2010, Sommer et al. 2012, Romagnan et al. 2015). In temperate and polar biomes, phytoplankton abundance varies from periods of proliferation in spring and autumn to periods of decline in summer and winter. In subtropical and tropical waters, where seasonal changes in solar radiation and temperature are less prominent, plankton abundance is more stable at an annual scale (Dakos et al. 2009). In the Mediterranean Sea, eukaryotic primary producers appear from early spring with the following sequence: pico-eukaryotes, silicoflagellates, diatoms and dinoflagellates (Romagnan et al. 2015).

APS has been widely described in marine ecosystems, leading to a variety of potential explanations often based on mechanisms such as bottom-up to top-down controls (Sverdrup 1953, Margalef 1978, Sommer et al. 1986, Behrenfeld 2010, Sommer et al. 2012, Smyth et al. 2014, Romagnan et al. 2015, Atkinson et al. 2018). Gilbert et al. (2012), Romagnan et al. (2015) and Barton et al. (2015) have provided evidence for a strong influence of the physical environment on phytoplankton dynamics, suggesting a bottom-up control of annual succession. A substantial impact of species interaction (i.e. grazing) imposing a top-down control (e.g. mesozooplankton species on protists) has also been suggested in the western part of the English Channel, however (Kenitz et al. 2017, Fileman et al. 2010).

The seasonal cycles of irradiance, temperature and stratification and the associated changes in pycnocline, thermocline and halocline are known to be closely associated with the onset of phytoplankton growth (Longhurst 1998), and nutrients influence the extent of the phytoplankton bloom (Sommer et al. 2012). Although APS starts typically by the onset of the spring bloom in most extra-tropical regions, winter is a key period preparing the ingredients needed to trigger the start of phytoplankton proliferation (Sommer et al. 2012). During winter, oceans and seas lose heat from their surface waters, which become denser and consequently start to sink (Mann and Lazier 1996). Wind intensifies oceanic turbulence, which in turn brings nutrients (nitrate, phosphate and silicic acid) in the euphotic zone (Falkowski and Oliver 2007) while diluting phytoplankton in the water column (Behrenfeld 2010).

According to the Sverdrup's model (Sverdrup 1953), the spring phytoplankton bloom can develop when the Mixed Layer Depth (MLD), which can reach several hundred meters in the North Atlantic Ocean during winter (Reygondeau and Beaugrand 2010), is shallower than a critical depth at which the integral of net growth rate becomes zero over the water column. Sverdrup's theory has greatly stimulated research and this hypothesis is applicable to both deep waters and off-shore environments but not in shallow coastal systems (Behrenfeld 2010, Sathyendranah et al. 2015, Lévy 2015). The intensity of the phytoplankton bloom is strengthened when solar heating and reduced winds increase vertical stratification, leading to a strong thermocline. Irradiance is an important factor due to its influence on critical depth and vernal stratification, allowing species to remain in the euphotic zone. It has also been observed that the phytoplankton bloom sometimes starts before water stratification, which has led some authors to challenge Sverdrup's concept (Behrenfeld 2010). For instance, the dilution-recoupling hypothesis from Behrenfeld (2010) explains how the spring phytoplankton bloom is the result of an increase in growth at a time of strong dilution of grazers in the water column due to the absence of stratification. Progressive stratification during the bloom reinforces the coupling between phytoplankton and grazers, and

the reduction in nutrients availability - combined to a high grazing pressure - induces bloom termination. When the mixed layer deepens and increases macro-nutrients concentration in the euphotic zone, an autumn phytoplankton bloom can occur (Longhurst 1998); it ends rapidly, however, because of light limitation (Sverdrup 1953, Geider et al. 2014).

The main objective of this study is to reconstruct APS using models of increasing complexity generated from the Macro-Ecological Theory on the Arrangement of Life (METAL; Beaugrand 2015) that consider a set of environmental parameters known to influence marine phytoplankton dynamics such as temperature, photosynthetically active radiation and macro-nutrients. METAL unifies together behavioural, physiological, phenological, biogeographic and long-term community shifts and consequently allows one to predict how communities form and how they are altered by environmental fluctuations, including climatic variability and global climate change (Beaugrand et al. 2010, 2013a, 2014, 2018). The strength of this approach is to consider that, even though ecosystems are complex adaptive systems, basic organisation and sensitivity of communities can be predicted from simple founding principles. A significant proportion of the spatial and temporal adjustments of marine communities are deterministic, being thereby intelligible, which opens the way to testable predictions. In this study, our objectives are to test whether APS is related to the interaction between the ecological niche (*sensu* Hutchinson 1957) of species and seasonal fluctuations in their environment, and to identify the key ecological dimensions of the niche that control the annual phytoplankton dynamics.

Here, using data from the Continuous Plankton Recorder (CPR) survey (Reid et al. 2003), we first characterise APS in the North Sea. We model this phenomenon using METAL and compare observed and predicted patterns. We then investigate how natural environmental fluctuations drive phytoplankton seasonality from initiation to termination. Finally, we discuss our results in the context of APS (Widdicombe et al. 2010, Sommer et al. 2012, Romagnan et al. 2015), including hypotheses that have been proposed to explain the spring bloom such as the critical depth and turbulence hypotheses (Sverdrup 1953, Huisman et al. 1999), dilution-recoupling hypothesis (Behrenfeld 2010), and net heat flux hypothesis (Smyth et al. 2014).

## **2. MATERIALS AND METHODS**

### **2.1. Biological data**

Biological data originated from the Continuous Plankton Recorder (CPR, <https://www.cprsurvey.org/data/our-data/>) survey. This marine biological monitoring programme, currently operated by the Marine Biological Association (MBA), has sampled the North Atlantic Ocean and its adjacent seas on a routine monthly basis since 1946 at a depth of approximately 7-10 meters (Reid et al. 2003). Data from this programme have been extensively used to (i) investigate APS (e.g., Colebrook 1979, 1982c, Zhai et al. 2013, Barton et al. 2015), (ii) characterise pelagic biodiversity (e.g., Beaugrand et al. 2002, Barnard et al. 2004), (iii) document distributional, phenological and physiological responses of marine species to climate change (e.g., Helaouët and Beaugrand 2009, Beaugrand et al. 2009, Thackeray et al. 2016, Beaugrand and Kirby, 2018) and (iv) anticipate the consequences of global warming in the pelagic realm (e.g., Reid et al. 1998, Beaugrand et al. 2015).

In this study, we restricted our analyses to phytoplankton communities in the North Sea (1°E - 4°E and 54°N - 56°N; Fig. S1) and considered 90 species or taxa commonly monitored by the CPR survey over the period 1946-2016 (Table S1). The area was chosen because it was regularly sampled over the last decades and is located relatively far from the coastline. In the selected area and for all selected taxa, we calculated a climatology for each Julian day (i.e. 365) by averaging the selected taxa abundances over the period 1958-2016.

## 2.2. Environmental data

Nutrients data originated from the World Ocean Atlas 2013 V2, provided by NOAA National Centers for Environmental Information (NCEI), Silver Spring, Maryland, USA (<https://www.nodc.noaa.gov/OC5/woa13/woa13data.html>) (Locarnini et al. 2013). It is a scientifically quality-controlled database of selected historical *in situ* surface and subsurface oceanographic measurements for phosphate ( $\mu\text{mol. L}^{-1}$ ), silicate ( $\mu\text{mol. L}^{-1}$ ) and nitrate ( $\mu\text{mol. L}^{-1}$ ). Monthly means are provided for these three parameters, on a 3D grid of 1° latitudes by 1° longitude by 37 depth levels. Here, we calculated the average nutrients concentration in the North Sea (1°E - 4°E and 54°N - 56°N; Fig. S1) for the first 20m. From this dataset, we calculated the N/P ratio (Redfield 1958), which is known to modulate APS (Falkowski et al. 2000).

We used the Photosynthetically Active Radiation (PAR;  $\text{Einstein} \cdot \text{m}^{-2} \cdot \text{day}^{-1}$ ), solar radiation spectrum in the wavelength range of 400-700 nm, as a proxy of the level of energy that can be assimilated by photosynthetic organisms (Asrar, Myneni & Kanemasu, 1989). PAR regulates both the composition and evolution of marine ecosystems, influencing the growth of phytoplankton and in turn the development of zooplankton and fish. Data were provided by the Giovanni online data system, developed and maintained by the NASA GES DISC ([http://gdata1.sci.gsfc.nasa.gov/daac-bin/G3/gui.cgi?instance\\_id=ocean\\_month](http://gdata1.sci.gsfc.nasa.gov/daac-bin/G3/gui.cgi?instance_id=ocean_month)). A monthly climatology of PAR at a spatial resolution of 9 km was carried out by compiling data of the Sea-viewing Wide Field-of-view Sensor (SeaWiFS) from 2009 to 2012.

Because of the well-known influence of temperature (Beaugrand et al. 2018), we assessed the thermal environment of the 90 phytoplankton species over our region of interest using Sea Surface Temperature (SST) from the Optimum Interpolation (OI), which is based on both *in situ* and satellite observations (see Reynolds et al. 2002 for a full description of the OI analysis). In contrast to other environmental data which were only available at a monthly resolution, we used daily SST for a finer estimation of the thermal preferendum of species. We first calculated daily SSTs on a 1° by 1° grid from January 1982 to December 2017 and data were then averaged in the area ranging from 1°E to 4°E and from 54°N to 56°N (Fig. S1). Annual changes in the environmental parameters are shown in Fig. 1.

## 2.3. Examination of APS from the CPR survey

First, we removed species that had average annual abundance < 0.5 in the target area (Table S1, Fig. S1). This procedure led to the selection of 81 phytoplankton species (Table S1) for which we estimated average daily abundances over the region of interest for the period 1946-2015. To minimise short-term fluctuations and reduce the noise inherent to these data, we applied an order-6 symmetrical moving average on each daily time series (Legendre and Legendre 1998).

A standardised Principal Component Analysis (PCA; Jolliffe 1986) was applied on the correlation matrix 81 phytoplankton species x 365 days and the first three principal components

(PCs) were examined to identify changes in annual succession. Species were then sorted according to their phenology by using normalised eigenvectors, i.e. linear correlation values with the corresponding PCs higher than |0.5| (Table S1). Only significative axes (PCs) were represented (Fig. 2).

Finally, we clustered phytoplankton species into five groups: Bacillariophyceae, Dinophyceae, Primmnesiophyceae, Dictyochophyceae and Cyanophyceae.

#### 2.4. Generation of pseudo-species using models from the METAL theory

We modeled patterns of APS using METAL (Beaugrand et al. 2014, 2018). First, we generated a pool of uni-dimensional niches (i.e., niches with only one ecological dimension) by using a Gaussian model (Ter Braak 1996):

$$A = c e^{-\left(\frac{(x-x_{opt})^2}{2t^2}\right)} \quad (1)$$

where A is the abundance of a species as a function of the value of a given environmental parameter x; c is the maximum abundance of a pseudo-species with c being fixed to 1 (Beaugrand, 2015);  $x_{opt}$  is the environmental optimum (e.g. the best environmental condition for a given species that can reach the highest level of abundance) and t is the ecological amplitude of a pseudo-species (i.e. the environmental range where a species can occur) for a given environmental factor (Table S3). Species abundance along environmental gradients is generally modelled using a Gaussian model (Gauch et al. 1974).

Multi-dimensional niches (i.e., niches with 2 or more ecological dimensions) were modelled as follows:

$$A = C e^{-\frac{1}{2} \left[ \left( \frac{x_1 - x_{opt1}}{t_1} \right)^2 + \dots + \left( \frac{x_n - x_{optn}}{t_n} \right)^2 \right]} \quad (2)$$

with  $2 \leq n \leq 5$  ecological dimensions,  $x_1$  to  $x_n$  the values of the environmental parameters,  $x_{opt1}$  to  $x_{optn}$ , the optimum values of  $x_1$  to  $x_n$ , and  $t_1$  to  $t_n$ , the ecological amplitudes of  $x_1$  to  $x_n$ .

Our simulations were based upon six environmental parameters: (i) SST, (ii) PAR, (iii) nitrate, (iv) phosphate, (v) silicate, and (vi) N/P ratio. When the N/P ratio was considered, neither nitrate nor phosphate concentrations were included in the models to avoid possible bias related to multicollinearity. We performed simulations using all possible environmental combinations from one to five ecological dimensions (Table S2), leading to a total of 84 runs (i.e. simulations): 16 uni-dimensional runs, 23 two-dimensional runs, 29 three-dimensional runs, 13 four-dimensional runs and 3 five-dimensional runs (Table S2). The characteristics (optimum and ecological amplitude) of all niches are presented in Table S3. For example, for temperature, we defined 7 optimum values (i.e. values corresponding to the highest abundance for a given pseudo-species) ranging from 0 to 36°C by increment of 6°C and 4 ecological amplitudes from 1 to 10°C by increment of 3°C, leading to the creation of 28 (4 x 7) virtual (or pseudo-) niches.

For each run, a large number of niches (from 21 to 15,431,472) was created (Table S3). To determine the total number of niches per run, we multiplied the number of niches generated for a

given dimension by the number generated for all other ecological dimensions. For example, for a run based on temperature, PAR and nitrate (i.e. a three-dimensional run), the total number of niches was  $28 \times 21 \times 27 = 15,876$  ecological niches (with 28 niches for SST, 21 for PARc and 27 for nitrate; Table S3).

To test whether the resolution of niches (i.e. the number of points along the niches) affected our analyses, we compared two extreme cases of uni-dimensional models (i.e. low and high resolutions) using each ecological variable. We added the term “bis” after the name of the variable to identify high-resolution niche (Tables S3-S4). When the word ‘bis’ was absent, the uni-dimensional niche had a low resolution. Because of the high number of categories generated in the high-resolution case (e.g. 144,648,000 categories for a run based on temperature bis, PARa bis and phosphate bis), we did not perform high-resolution analyses based on more than one dimension because of calculation time estimated to be ~4 months on a high-performance computer of 88 cores.

To examine the sensitivity of our analyses to low PAR values, we considered three minimum values: 1 (termed “PARa”, Table S3), 10 (“PARb”) and 20 (“PARc”)  $\text{E.m}^{-2}.\text{day}^{-1}$ .

Finally, annual estimations of pseudo-species abundances were assessed by performing a cubic interpolation of the 1-5D niches with the corresponding environmental variables. Four runs on APS are closely examined as examples: (i-iii) three uni-dimensional runs based on either (i) SST, (ii) PAR or (iii) nitrate (Fig. 3) and (iv) one three-dimensional run based on SST, PAR and nitrate (Fig. 4).

## 2.5. Comparisons of predicted and observed seasonal patterns

Comparisons between predicted and observed annual patterns in phytoplankton abundance were performed in two ways. First, we calculated the coefficient of linear correlation (Pearson’s correlation coefficient; Fig. 5 and Fig. S3). Second, we used the Mean Absolute Error (MAE; Fig. S3) that measures the average magnitude of the errors in a set of predictions, without considering their direction.

$$MAE = \sum_{i=1}^n \frac{|X_i - Y_i|}{n} \quad (3)$$

with  $n$  the number of differences to be tested,  $X_i$  is prediction  $i$  and  $Y_i$  is observation  $i$ . Equation (3) represents the absolute differences between predictions and observations, divided by the number of differences to be tested (with all individual differences having equal weight). It is a negatively-oriented score, which means that the lower values are related to the strongest correlations.

Pearson’s correlation coefficients and MAEs were calculated for each run between all observed and predicted daily patterns in (pseudo-) species abundance, leading to a correlation or MAE matrix  $u \times v$  (species  $\times$  pseudo-species). We then identified the highest positive correlations and the lowest MAE values. For each run, we therefore obtained two vectors using the average correlation and MAE values calculated for each species (Fig. S4). The daily normalised (between 0 and 1) pseudo-species abundances that showed the highest correlation with observed species were plotted against daily observed species abundances to graphically depict the relationships (Fig. 5).

We then tested both correlations and MAEs using null models that considered (or not) temporal autocorrelation. First, we randomly generated a number of daily time series



corresponding to the total number of pseudo-species generated for each run. Although the number of time series was small for 1D runs, it became important when the number of dimensions increased as we multiplied the number of niches per parameter. The procedure was repeated 1000 times and, for each simulation, the average correlation and MAE values were calculated. To consider temporal autocorrelation, we generated two million of time series and kept the first 1000 with a 30-order (i.e., 30 days/~one-month autocorrelation for daily time series) autocorrelation higher than average 30-order autocorrelation found in observed daily time series. We represented the results in a diagram that exhibited the observed average correlation for each run and the 1000 correlations found using the null model with (red) and without (blue) autocorrelation (Fig. S3). For each combination of environmental variables (i.e. 84 runs), we calculated the probability of significance of each correlation (Table S4). Finally, we used contour diagrams to identify (i) the most important environmental parameters and (ii) the number of dimensions to accurately reconstruct APS. This graphical examination allowed us to highlight the number of species that exhibits the highest correlations in each run (Fig. 6).

### **3. RESULTS**

#### **3.1. Seasonal changes in environmental parameters in the North Sea**

Temperature exhibited a minimum at the beginning of March and a maximum at the end of July-August (Fig. 1). PAR showed minimum and maximum values in December-January and June, respectively. The highest concentrations in nitrate, phosphate and silicate were observed in winter and reached their lowest concentrations from the end of spring to the end of summer. Except for SST, no variation was captured within a given month because monthly means were used for all other parameters.

#### **3.2. Observed annual phytoplankton succession**

We examined APS based on CPR plankton data by means of a PCA (Fig. 2). The use of the first three principal components allowed us to differentiate five periods, each being characterised by a species assemblage: (i) an early-spring stage (Fig. 2b left part of the panel, 8 species negatively correlated to PC1), (ii) a spring stage (Fig. 2c, 22 species positively correlated to PC2), (iii) a widespread summer stage (Fig. 2a, 28 species positively related to PC1), (iv) a late summer/beginning of autumn stage (Fig. 2d, 13 species negatively correlated to PC3) and (v) an autumn stage (Fig. 2b right part of the panel, 8 species negatively correlated to PC1). The summer stage (Fig. 2a) was characterised by the highest species richness, but showed a low proportion of diatoms in comparison to both spring or autumn stages; silicoflagellates were also present (Table S1). Other principal components were not represented because they did not bring additional information.

#### **3.3. Modelled annual phytoplankton succession**

We reconstructed APS by using models of growing complexity (i.e., by considering a growing number of niche dimensions) including all combinations of SST, PAR, nitrate, phosphate, silicate and N/P ratio (a total of 84 runs). Here, we focused on four examples of modelled APS reconstructed by using different ecological dimensions (Fig. 3 and 4). The first run, based on SST only, showed two main phases of high phytoplankton abundance (also representative of a high species richness) in summer (Fig. 3a) and winter (Fig. 3b) and two minor phases in spring (Fig.

3c) and autumn (Fig. 3c). The winter phase of high abundance did not correspond to any observed patterns (Fig. 2 *versus* Fig. 3). The second run, based on PAR only, showed several peaks of high phytoplankton abundance in spring, summer and autumn (Fig. 3d-f). These patterns were close to observed patterns of annual succession (Fig. 2), suggesting an important role of PAR in the modulation of APS. The third model, based on nitrate only (Fig. 3g-i), showed an important winter peak in phytoplankton abundance, not detected in the observations (Fig. 2 *versus* 3). This result suggests that considering nitrate only was not sufficient to reconstruct APS. The fourth model, that combined SST, PAR and nitrate (Fig. 4a-e), was more efficient to reproduce APS observed in the CPR data, especially the late-summer phase (Fig. 4 *versus* Fig. 2). A closer examination of the relationships between predicted and observed APS is performed below.

### **3.4. Relationships between observed and modelled annual phytoplankton succession**

#### **3.4.1. Reconstruction of species seasonal patterns**

We calculated the Pearson's correlation coefficients between observed and simulated (pseudo-) species for all 84 runs; we remind here that our runs were characterised by a growing number of ecological dimensions - ranging from one to five - and that all combinations (C=84) of environmental parameters were tested. We chose the best correlations and examined graphically the relationships between observed and predicted phytoplankton abundances (Fig. 5). Figure 5 shows all the relationships between phytoplankton species considered in the analyses and pseudo-species created from METAL. For all phytoplankton groups, simulated pseudo-species reproduced observed seasonal patterns well: most annual phytoplankton patterns in observed and simulated phytoplankton species were closely related (e.g., *Skeletonema costatum* and *Thalassiosira* spp.) with the exception of *Paralia sulcata* and *Dactyliosolen antarcticus* (Fig. 5). Correlation and MAE values are examined in detail in the following sections.

#### **3.4.2. Identification of key ecological dimensions to reconstruct APS**

To identify key ecological dimensions, we calculated the average of the best correlations and MAEs between observed and simulated (pseudo-) species for all 84 runs (Table S4, Fig. S3). We tested our correlations and MAEs using a null model with and without consideration for temporal autocorrelation. While some MAE values were significant for some 1D runs (Fig.S3), APS was better reproduced when at least three dimensions were considered (Fig. S3). Not all correlations were significant for models based on three or more ecological dimensions while considering five dimensions did not improve the percentage of explained variance (i.e. model quality). This suggests that the selection of relevant environmental variables is more important than considering a too high number of ecological dimensions.

#### **3.4.3. Identification of key environmental variables to reconstruct APS**

We then identified the most relevant environmental parameters and the number of ecological dimensions that best reproduce APS (Fig. 6). We remind here that APS is the result of species phenology (i.e., species seasonal patterns). Uni-dimensional models (1D, Runs 1-16) explained poorly observed seasonal changes in species abundance, with the exception of Run 2 that was exclusively based on SST (Fig. 6a); for Run 2, eight species showed their highest correlations between observed and modelled seasonal patterns. Bi-dimensional models (Runs 17-39) also explained poorly species seasonal patterns and only 3 species exhibited their highest correlations when the model was based on both temperature and PAR (Fig. 6a, Table S2). Better results were

achieved when models were based on three or more ecological dimensions. Three-dimensional models (Runs 40-68) had 29 highest correlations between observed and modelled seasonal patterns (Fig. 6a). Run 51 based on SST, N/P and PARc (i.e., a minimum value of  $PAR=20 \text{ E.m}^{-2}.\text{day}^{-1}$ ) exhibited 10 highest correlations. Four-dimensional (Runs 69-81) and five-dimensional models (Runs 82-84) had 25 and 14 highest correlation values, respectively.

We also examined the correlations between each simulated and observed seasonal patterns for all species and runs (Fig. 6b). The figure showed that even if best results were achieved for models based on SST only (Run 2), results were similar when three or more dimensions were included. Low correlations generally appeared when the triplet SST/PAR/macro-nutrient was not used (Fig. 6b and Table S2, e.g., Runs 53-56), revealing that the combination of these variables was important to reproduce most species seasonal patterns.

## 4. DISCUSSION

### 4.1. Annual phytoplankton succession

The METAL theory suggests that large-scale patterns in biodiversity emerged from the niche-environment interactions that propagate from the species to the community level (Beaugrand et al. 2013b, Beaugrand et al. 2015, Beaugrand et al. 2018). Here, our results show that APS - including the spring bloom - may also originate from the niche-environment interaction (Fig. 5). APS has been frequently investigated at the group level (e.g. plankton functional type, plankton ecology groups or categories). However, our study shows that even within a given ecological or taxonomic group, species reacts to environmental fluctuations individually through the niche-environment interaction, conforming themselves to the principle of species individuality (Whittaker 1975) (Fig. 5). Our study therefore suggests that it is important to investigate APS by exploring ecological patterns and processes at a species level.

Our results show a prominent control of APS by environmental conditions in the North Sea. Studying APS in the Mediterranean Sea, Romagnan et al. (2015) have also provided evidence for a strong control of the physical environment on APS. Even though our modelling approach reproduced well the seasonal cycle of eight species when based on SST only, better results were achieved when three or more ecological dimensions were considered (Fig. 6). Considering five dimensions did not improve substantially the percentage of explained variance, probably because seasonal changes in nitrate, phosphate and silicate concentrations are highly correlated in the North Sea.

Our investigation of APS revealed four main microphytoplanktonic succession in the North Sea (see Table S1 for a list of the species considered in our study). The first assemblage is composed of species that exhibited their highest abundance at the beginning of spring and a second less important peak in autumn (PC1 in Fig. 2b, Fig. 5). This microphytoplanktonic assemblage, generally composed of large diatoms (Table S1 and Fig. 5, e.g. *Thalassionema nitzschioides*, *Ditylum brightwellii*), was primarily controlled by PAR and nutrients availability in our models. PAR is an essential parameter limiting photosynthesis and its influence on growth rate is well known (Eppley & Sloan, 1966). PAR is a strong limiting factor in areas above the polar circle (McMinn & Martin, 2013) but also in lower latitude regions such as the North Sea (Peeters et al.

1993). Nutrients positively influenced growth rate and primary production (Goldman 1980, Longhurst 1998). The first assemblage is also psychrophilic, reaching its highest abundance when temperature is lowest and their lowest abundance when temperature is highest (Fig. 1). The assemblage is not detected when PAR is highest and when PAR or nutrients concentration is lowest (Fig. 1). Although not considered in our analyses, turbulence, mixing and high SST variability that characterise early spring and autumn may also positively influence the occurrence of this assemblage, which is more adapted to such an environment than dinoflagellates (Beaugrand et al. 2010, Holligan et al. 1980, Margalef 1978). In winter, PAR (or the number of daily light hours) and to a lesser extent temperature limit diatom growth and deep-water column mixing combined to an absence of biological production enable nutrients to increase at the sea surface.

The second assemblage (e.g. *Chaetoceros* spp., *Coscinodiscus concinnus*) occurs generally between April and June at a time when silicate and to a lesser extent nitrate and phosphate concentrations diminish and temperature and PAR increase (Fig. 1, 2c and 5). This assemblage is less psychrophile than the first one and occur at a time when both temperature and PAR increase (Fig. 1).

The third assemblage is composed of species, mainly dinoflagellates (e.g. *Ceratium fusus* and *C. furca*) and some small diatoms (e.g. *Guinardia striata*, *G. flaccida*), occurring when temperature and PAR are high and conditions are oligotrophic (Fig. 1, 2a and 5). Silicate depletion played an important role in the change of dominance observed between the second and the third assemblage. In a mesocosm experiment, silicate deficiency was assumed to be the cause of the strong reduction in large spring bloom diatoms and the replacement by flagellates (Jacobsen et al. 1995). Small diatoms need less silicic acid for the their skeleton and have a higher surface to volume ratio which increases nutrient absorption (Miller, 2004). Dinoflagellates occur in areas and at time when both temperatures are warm, SST variability low and the water column is well stabilised (Beaugrand et al. 2010, Margalef 1978).

The fourth assemblage is composed of species (e.g. the diatom *Belleriochea malleus*, *Biddulphia alternans*) having their occurrence from August to October (Fig. 2d and 5). Those species occur when temperature is high and when nutrients concentration tends to increase. Those warm-temperate species have their northern limit of spatial distribution in the North Sea (e.g. *Belleriochea malleus*)(Barnard et al. 2004).

Despite the fact that four main microphytoplanktonic successions were identified by the PCA, many intermediate situations occur (Fig. 5). For example, some species (e.g. *Rhizosolenia setigera*) exhibit a higher abundance when PAR are above  $10 \text{ E.m}^{-2}.\text{day}^{-1}$  but show a diminution when temperature is high and conditions are oligotrophic (Fig. 5). A summer reduction is sometimes not observed for species occurring between spring and autumn (e.g. *Gyrosigma* spp.). Some species have a peak in late spring and another smaller one in autumn (e.g. *Dactyliosolen fragilissimus*). Others have a small peak in spring and a high one in autumn (e.g. *Leptocylindrus danicus*). Many species have narrow seasonal peaks not identified by the PCA (e.g. *Asteromphalus* spp., *Ceratium buceros*, *C. carriense*). Because most observed patterns in annual abundance were well reconstructed by our approach, it is likely that APS may result from the niche-environment interaction (Fig. 5). Sharp or gradual environmental gradients interact with the niche of each species within a multidimensional space to generate a variety of phenological patterns (Fig. 5).

The application of the Plankton Ecology Group (PEG) model in lakes and subsequently in the marine realm (Sommer et al. 1986, Sommer et al. 2012) has suggested that (i) physics (light and stratification) controls the start and the end of the phytoplankton growth season, (ii) grazing by metazoan plankton results in a clear water phase, (iii) nutrients define the carrying capacity of phytoplankton, (iv) food limitation determines zooplankton abundances and (v) fish predation determines zooplankton size structure. The PEG model has emphasised the role of physical factors, grazing and nutrient limitation for phytoplankton. Our results have shown the key role of bottom-up processes in shaping APS and recall the importance of considering a combination of several environmental factors, not only light. PAR and to a lesser extent SST, are important for the initiation of the spring bloom, macronutrients for the end of the spring bloom and both SST and macronutrients for the development of APS. Light (e.g. PAR, photoperiod), nutrients and temperature are seen as master parameters controlling photosynthesis in physiological studies (Geider et al. 1997, Longhurst 1998, McMinn & Martin 2013, Ras et al. 2013). While grazing may have a substantial influence (Kivi et al. 1993, Fileman et al. 2010, Kenitz et al. 2017), the absence of grazing consideration in our analyses did not prevent us to accurately reconstruct species phenology (Fig. 5).

#### **4.2. The spring bloom**

Our study also provides evidence for a strong environmental control of the initiation, development and termination phases of the spring bloom although processes are distinct from those formulated by Gran and Braarud (Gran and Braarud 1935) and Sverdrup (1953). The Critical Depth Theory (Sverdrup 1953) proposed that spring blooms in regions close to the North Atlantic Drift Provinces develop when the Mixed Layer Depth (MLD) becomes shallower than the critical depth (i.e., blooming can occur when MLD is less than the critical value), which was derived analytically as a function of the amount of incoming radiation, water transparency and the energy level at the compensation depth (i.e., the depth at which gross photosynthesis balances phytoplankton respiration). According to the CDT, bloom initiation is only possible in spring in high latitudes.

The possibility that the onset of the spring phytoplankton bloom occurs as a consequence of decreased zooplankton grazing pressure has recently been proposed by Behrenfeld (2010). Our models suggest that neither the occurrence of a MLD shallower than the critical depth nor a dilution effect resulting from the occurrence of a deep MLD is necessary to reproduce bloom initiation and more generally species phenology in the investigated North Sea region. The integration of PAR - and to a lesser extent SST - in the models simply explained the initiation of the spring bloom in the North Sea. Average light intensity in the mixed layer is well-known to govern the timing of the spring bloom (Riley 1967; Legendre 1990), even if phytoplankton production losses due to mixing may also be important (Behrenfeld 2010). Some studies have also reported that spring bloom may occur in the absence of water stratification (Townsend et al. 1992), confirming that phytoplankton initiation may precede the establishment of a clear thermocline (Colebrook 1979). Revisiting the dilution-recoupling hypothesis (Behrenfeld 2010), Beaugrand (2015) has also suggested PAR as a key driver of bloom initiation (his figure 5.27). Smyth and colleagues (2014) have conveyed that the spring bloom started in the western part of the English Channel (Station L4, Plymouth) when net heat flux becomes positive. Because net heat flux is highly positively related to irradiance and PAR (Beaugrand 2015), a strong control of PAR on the initiation of the spring bloom may be expected.

Our models also suggest that the limitation in macro-nutrients is a key factor for bloom termination, which is only in partial agreement with the Sverdrup and the Behrenfeld hypotheses. To model the end of the spring bloom, we did not have to include grazing (Sverdrup 1953) or a coupling between grazers and phytoplankton (Behrenfeld 2010). Instead, the low macro-nutrients concentrations could explain alone bloom termination. As earlier, we do not state that grazing has not an effect, but we suggest that the physical environment is an important driver. Large seasonal changes in atmospheric forcing and ocean surface conditions shape, to a great degree, the seasonal cycles of phytoplankton biomass, but also the relative abundance of phytoplankton species (Barton et al. 2014). Beaugrand (2015) showed that phytoplankton and zooplankton seasonal fluctuations were closely related in the North Atlantic region investigated by Behrenfeld (his figure 5.28), suggesting a “bottom-up” control. More recently, Atkinson and colleagues (2018) demonstrated that both the increase and termination of the spring bloom are encapsulated by zooplankton, providing strong evidence against a top-down control.

Although the succession between diatoms and dinoflagellates can be well explained by macro-nutrients and temperature in our models, it is well-known since Margalef (1979) that water column stability is a key factor to explain the succession between these two functional groups. Dinoflagellates are more sensitive than diatoms to turbulence (Karp-Boss et al. 2000). They can realise significant vertical migration to nutrient rich area but cannot reproduce when turbulence is too high (Estrada and Berdalet 1997). In contrast, diatoms can continue cell division and the photosynthetic energy products are used to synthesize fatty acid that are converted to energy when cells are exported below the euphotic zone; fatty acid can be considered as a buoyancy regulator (Amato et al. 2017). It is possible that mixing and turbulence are not required in our models because temperature is a proxy of mixing and turbulence conditions in the North Sea. Confirmation of our results should be searched in other regions experiencing different sequences of environmental conditions.

#### **4.3. Uncertainties related to our approach**

The niche-environment interaction is certainly more unpredictable in the field than in our modelling approach for two main reasons. First, while the fundamental niche (*sensu* Hutchinson) was estimated here, the environment - through random meteorological conditions - may influence the realised niche of microalgae species. Second, phytoplankton community before and/or during the growth of a given species may alter species realised niche by competition for resources that lead to competitive exclusion. The trait-based approach of Breton et al. (2017) suggests that competitive exclusion prevails during *Phaeocystis* spp. bloom.

It is well-known that the underwater light available for photosynthesis (PAR) is a key environmental variable for primary production (Cole and Cloern 1987, MacIntyre et al. 2000, Foden et al. 2010, Capuzzo et al. 2013, 2015, 2018). Light field in the water column depends in turn on phytoplankton biomass (self-shading), inorganic suspended particulate materials, colored dissolved organic materials and water itself (IOCCG 2000). Recent works on light quality have also revealed the important role of spectral irradiance on phytoplankton succession (Lawrenz and Richardson 2017). In this study, we used surface PAR data that originated from a climatology. All phytoplankton species can perform photo-regulation or photo-acclimation (i.e., the first occurs at time scales of minutes and the second takes place in a few hours or a day) to limit photo-inhibition in high light surface waters or optimise both light harvesting and Calvin cycle activity in the water column (MacIntyre et al. 2000, Lavaud 2007, Dubinsky and Stambler 2009). In addition, photo-

acclimation processes can be conducted on different kinetic models and time scales (Cullen and Lewis 1988), according to environmental conditions and functional phytoplankton groups (MacIntyre et al. 2000). Even if photosynthesis performances between different species remain poorly documented (Goss et Lepetit 2015, Suggett et al. 2015), they can induce a competitive effect between species at a given time.

## 5. CONCLUSIONS

Our study suggests that APS may result from the niche-environment interaction. Our model provides evidence that sharp temporal environmental gradients may be responsible for the strong annual shifts in microphytoplanktonic composition in the North Sea; this occurs when an environmental factor becomes rapidly favourable (e.g. increasing PAR at the end of winter) or limiting (e.g. diminution of macro-nutrients at the end of spring). We identify three key parameters that influence directly the succession: (i) temperature, (ii) PAR and (iii) macro-nutrients. There is a clear effect of temperature on APS with a cline from cold-water species in early spring to warm-water species in late summer. By enabling the initiation of the spring bloom and ending the second bloom in autumn, PAR exerts an important role. Macro-nutrients are critical at the end of the spring bloom and their increases in autumn trigger a secondary bloom which then becomes rapidly limited by PAR and temperature. Mixing is an important process by which macro-nutrients increase in the euphotic zone. In the light of our results the shoaling of the pycnocline should not be directly involved in bloom initiation (i.e., Sverdrup's hypothesis), however, and the increase in grazing is not determinant for its termination (Behrenfeld's hypothesis).

## 6. Acknowledgements

The CPR Survey is an internationally funded charity that operates the CPR programme. The CPR survey operations and routes are funded by a funding consortium from the UK, USA, Canada and Norway. Within the UK, government organisations DEFRA and NERC contribute to core operations. Part of this research was funded by the Centre National de la Recherche Scientifique (CNRS). This research was funded as part of the ANR TROPHIK.

## References

- Amato, A., Dell'Aquila, G., Musacchia, F., Annunziata, R., Ugarte, A., Maillet, N., Carbone, A., Ribera d'Alcalà, M., Sanges, R., Iudicone, R., and Ferrante, M. 2017. Marine diatoms change their gene expression profile when exposed to microscale turbulence under nutrient replete conditions. *Scientific Report* 3826, 1–11.
- Asrar, G., Myneni, R. B., Li, Y., and Kanemasu, E. T. (1989). Measuring and modeling spectral characteristics of a tallgrass prairie, *Remote Sens. Environ.* 27:143-155.
- Assis, J., Tyberghein, L., Bosh S., Verbruggen, H., Serrão, E.A., De Clerck, O. 2017. Bio-ORACLE v2.0: Extending marine data layers for bioclimatic modelling. *Global Ecology and Biogeography* 27, 277–84.
- Atkinson, A., Polimene, L., Fileman, E.S., Widdicombe, C.L., McEvoy, A.J., Smyth, T.J., Djeghri, N., Sailley, S.F., Cornwell, L.E.. 2018. What drives plankton seasonality in a stratifying shelf

- sea? Some competing and complementary theories. *Limnology and Oceanography* 9999, 1–7.
- Barnard, R., Batten, S. D., Beaugrand, G., Buckland, C., Conway, D. V. P., Edwards, M., Finlayson, J., Gregory, L. W., Halliday, N. C., John, A. W. G., Johns, D. G., Johnson, A. D., Jonas, T. D., Lindley, J. A., Nyman, J., Pritchard, P., Reid, P. C., Richardson, A. J., Saxby, R. E., Sidey, J., Smith, M. A., Stevens, D. P., Taylor, C. M., Tranter, P. R. G., Walne, A. W., Wootton, M., Wotton, C. O. M., and Wright, J. C. 2004. Continuous plankton records: plankton atlas of the North Atlantic Ocean (1958–1999). II. Biogeographical charts. *Marine Ecology Progress Series Supplement*, 11–75.
- Barton, A. D., Lozier, M. S., and Williams, R. G. 2015. Physical controls of variability in North Atlantic phytoplankton communities. *Limnology and Oceanography* 60, 181–197.
- Beaugrand, G., Reid, P. C., Ibañez, F., Lindley, J. A. and Edwards, M. 2002. Reorganization of North Atlantic marine copepod biodiversity and climate. *Science* 296, 1692–1694.
- Beaugrand, G., Luczak, C., and Edwards, M. 2009. Rapid biogeographical plankton shifts in the North Atlantic ocean. *Global Change Biology* 15, 1790–1803.
- Beaugrand, G., Edwards, M., and Legendre, L. 2010. Marine biodiversity, ecosystem functioning and the carbon cycles. *Proceedings of the National Academy of Sciences* 107, 10120–10124.
- Beaugrand, G., Mackas, D., and Goberville, E. 2013a. Applying the concept of the ecological niche and a macroecological approach to understand how climate influences zooplankton: advantages, assumptions, limitations and requirements. *Progress in Oceanography* 111, 75–90.
- Beaugrand, G., Rombouts, I., and Kirby, R. R. 2013b. Towards an understanding of the pattern of biodiversity in the oceans. *Global Ecology and Biogeography* 22, 440–449.
- Beaugrand, G., Goberville, E., Luczak, C., Kirby, R.R. 2014. Marine biological shifts and climate. *Proceedings of the Royal Society B: Biological Sciences* 281, 20133350.
- Beaugrand, G. 2015. Marine biodiversity, climatic variability and global change. London: Routledge.
- Beaugrand, G., Edwards, M., Raybaud, V., Goberville, E., Kirby, R.R. 2015. Future vulnerability of marine biodiversity compared with contemporary and past changes. *Nature Climate Change* 5, 695–70.
- Beaugrand, G., 2015. Theoretical basis for predicting climate-induced abrupt shifts in the oceans. *Philosophical Transactions of the Royal Society B: Biological Sciences*, 370 20130264.
- Beaugrand, G., and Kirby, R. R. 2018. How do marine pelagic species respond to climate change? Theories and observations. *Annual Review of Marine Science* 10, 169–197.
- Beaugrand, G., Luczak, C., Goberville, E., Kirby, R.R. 2018. Marine biodiversity and the chessboard of life. *Plos One* 13, e0194006.
- Behrenfeld, M. J. 2010. Abandoning Sverdrup's Critical Depth Hypothesis on phytoplankton blooms. *Ecology* 91, 977–989.
- Breton, E., Christaki, U., Bonato, S., Didry, M., Artigas, L.F. 2017. Functional trait variation and nitrogen use efficiency in temperate coastal phytoplankton. *Marine Ecology Progress Series* 563, 35–49.
- Capuzzo, E., Painting, S. J., Forster, R. M., Greenwood, N., Stephens, D. T. and Mikkelsen, O. A. 2013. Variability in the sub-surface light climate at ecohydrodynamically distinct sites in the North Sea. *Biogeochemistry* 113, 85–103.



- Capuzzo, E., Stephens, D., Silva, T., Barry, J., and Forster, R. M. 2015. Decrease in water clarity of the southern and central North Sea during the 20<sup>th</sup> century. *Global Change Biology* 21, 2206–2214.
- Capuzzo, E., Lynam, C., Barry, J., Stephens, D., Forster, R. M., Greenwood, N., McQuatters-Gollop, A., Silva, T., van Leeuwen, S. M. and Engelhard, G. H. 2018. A decline in primary production in the North Sea over 25 years, associated with reductions in zooplankton abundance and fish stock recruitment. *Global Change Biology* 24, 352–364.
- Cole, B. E., and Cloern, J. E. 1987. An empirical model for estimating phytoplankton productivity in estuaries. *Marine Ecology Progress Series* 36, 299–305.
- Colebrook, J. M. 1979. Continuous Plankton Records: seasonal cycles of phytoplankton and copepods in the North Atlantic Ocean and the North Sea. *Marine Biology* 51, 23–32.
- Colebrook, J. M. 1982. Continuous Plankton Records: seasonal variations in the distribution and abundance of plankton in the North Atlantic Ocean and the North Sea. *Journal of Plankton Research* 4, 435–462.
- Cullen, J. J., and Lewis, M. R. 1988. The kinetics of algal photoadaptation in the context of vertical mixing. *Journal of Plankton Research* 10, 1039–1063.
- Cushing, D. H. 1959. The seasonal variation in oceanic production as a problem in population dynamics. *Journal du Conseil* 24, 455–464.
- Dakos, V., Beninca, E., van Nes, E.H., Philippart, C.J.M., Scheffer, M., Huisman, J. 2009. Interannual variability in species composition explained as seasonally entrained chaos. *Proceedings of the Royal Society B* 276, 2871–80.
- Dubinsky, Z., and Stambler, N. 2009. Photoacclimation processes in phytoplankton: mechanisms, consequences, and applications. *Aquatic Microbial Ecology* 56, 163–176.
- Eppley, R.W., Sloan P.R., 1966. Growth rates of marine phytoplankton: correlation with light absorption by cell chlorophyll a. *Physiologia Plantarum* 19, 47–59.
- Estrada, M., and Berdalet, E. 1997. Phytoplankton in a turbulent world. *Scientia Marina* 61, 125–140.
- Falkowski, P., Scholes, R. J., Boyle, E., Canadell, J., Canfield, D., Elser, J., Gruber, N., Hibbard, K., Högberg, P., Linder, S., Mackenzie, F. T., Moore III, B., Pedersen, T., Rosenthal, Y., Seitzinger, S., Smetacek, V., and Steffen, W. 2000. The global carbon cycle: A test of our knowledge of Earth as a system. *Science* 290, 291–296.
- Falkowski, P. G., and Oliver, M. J. 2007. Mix and max: how climate selects phytoplankton. *Nature Reviews Microbiology* 5, 813–819.
- Fileman, E., Petropavlovsky, A., and Harris, R. 2010. Grazing by the copepods *Calanus helgolandicus* and *Acartia clausi* on the protozooplankton community at station L4 in the Western English Channel. *Journal of Plankton Research* 32, 709–724.
- Foden, J., Devlin, M. J., Mills, D. K., and Malcolm, S. J. 2010. Searching for undesirable disturbance: an application of the OSPAR eutrophication assessment method to marine waters of England and Wales. *Biogeochemistry* 106, 157–175.
- Gauch, H. G., Chase, G. B., and Whittaker, R. H. 1974. Ordination of vegetation samples by Gaussian species distributions. *Ecology* 55, 1382–1390.
- Geider, R.J., MacIntyre, H.L., Kana T.M. 1997. A dynamic model of phytoplankton growth and acclimation: responses of the balanced growth rate and chlorophyll a: carbon ratio to light, nutrient-limitation and temperature. *Marine Ecology Progress Series*, 148, 187–200.
- Geider, R. J., C. M. Moore, and D. J. Suggett 2014. Ecology of Marine Phytoplankton. *Ecology and the Environment. Springer* 1–41.

- Gilbert, J. A., Steele, J. A., Caporaso, J. G., Steinbrück, L., Reeder, J., Temperton, B., and Somerfield, P. J. 2012. Defining seasonal marine microbial community dynamics. *The ISME journal* 6, 298–308.
- Goldman, J. C., 1980. Physiological processes, nutrient availability, and the concept of relative growth rate in marine phytoplankton ecology. *Primary Productivity in the Sea*, ed. P. G. Falkowski, 179–194. New York: Plenum
- Goss, R., and Lepetit, B. 2015. Biodiversity of NPQ. *Journal of Plant Physiology* 172:13–32.
- Helaouët, P., and Beaugrand, G. 2009. Physiology, ecological niches and species distribution. *Ecosystems* 12, 1235–1245.
- Gran, H.H., Braarud, T. 1935. A quantitative study of the phytoplankton in the Bay of Fundy and the Gulf of Maine (including observations on hydrography, chemistry and turbidity). *Journal of the Biology Board of Canada*, 1 (5), 279–467.
- Holligan, P.M., Maddock, L., Dodge, J.D. 1980. The distribution of dinoflagellates around the British Isles in July 1977: a multivariate analysis. *Journal of Marine biology Association* UK, 60, 851–867.
- Huisman, J., van Oostveen, P., and Weissing, F. J. 1999. Critical depth and critical turbulence: two different mechanisms for the development of phytoplankton blooms. *Limnology and Oceanography* 44, 1781–1787.
- Hutchinson, G. E. 1957. Concluding remarks. *Cold Spring Harbor Symposium on Quantitative Biology* 22, 415–427.
- IOCCG. 2000. Remote sensing of ocean colour in coastal, and optically-complex, waters. *Reports of the International Ocean-Colour Coordinating Group, n°3*, edited by S. Sathyendranath, 140, Dartmouth.
- Jacobsen A., Egge J.K. and Heimdahl B.R. 1995. Effects of increased concentration of nitrate and phosphate during a spring bloom experiment in microcosm. *Journal of Experimental Marine Biology and Ecology* 187: 239–251.
- Jolliffe, I. T. 1986. Principal Component Analysis. Springer-Verlag New York Inc. *Springer series in statistics*.
- Karp-Boss, L., Boss, E., and Jumars, P. A. 2000. Motion of dinoflagellates in simple shear flow. *Limnology and Oceanography* 45, 1594–1602.
- Kenitz, K., Visser, A., Mariani, P., and Andersen, K. H. 2017. Seasonal succession in zooplankton feeding traits reveals trophic trait coupling. *Limnology and Oceanography* 62, 1184–1197.
- Kivi, K., Kaitala, S., Kuosa, H., Kuparinen, J., Leskinen, E., Lignell, R., Marcussen, B., and Tamrninen, T. 1993. Nutrient limitation and grazing control of the Baltic planktonic community during annual succession. *Limnology and Oceanography* 38, 893–905.
- Lavaud, J. 2007. Fast regulation of photosynthesis in diatoms: Mechanisms, evolution and ecophysiology. *Functional Plant Science and Biotechnology* 1, 267–287.
- Lawrenz, E., and Richardson, T. L. 2017. Differential effects of changes in spectral irradiance on photoacclimation, primary productivity and growth in *Rhodomonas salina* (cryptophyceae) and *Skeletonema costatum* (bacillariophyceae) in simulated black water environment. *Journal of Phycology* 53, 1241–1254.
- Legendre, L. 1990. The significance of microalgal blooms for fisheries and for the export of particulate organic carbon in oceans. *Journal of Plankton Research* 12, 681–699.
- Legendre, P., and Legendre, L. 1998. Numerical Ecology. 2<sup>nd</sup> edition. Elsevier Amsterdam.
- Lévy, M. 2015. Exploration of the critical depth hypothesis with a simple NPZ model. *ICES Journal of Marine Science* 72, 1916–1925.

- Locarnini, R. A., Mishonov, A. V., Antonov, J. I., Boyer, T. P., Garcia, H. E., Baranova, O. K., Zweng, M. M., Paver, C. R., Reagan, J. R., Johnson, D. R., Hamilton, M., and Seidov, D., 2013. World Ocean Atlas, Volume 1: Temperature, edited by: Levitus, S. and Mishonov, A., NOAA Atlas NESDIS 73, 40.  
Available at: [http://data.nodc.noaa.gov/woa/WOA13/DOC/woa13\\_vol1.pdf](http://data.nodc.noaa.gov/woa/WOA13/DOC/woa13_vol1.pdf).
- Longhurst A. 1998. Ecological geography of the sea. Academic Press, London
- MacIntyre, H. L., Kana, T. M., and Geider, R. J. 2000. The effect of water motion on short-term rates of photosynthesis by marine phytoplankton. *Trends in Plant Science* 5, 12–7.
- Mann, K. H., and Lazier, J. R. N. 1996. Dynamics of marine ecosystems: biological-physical interactions in the oceans. 2<sup>nd</sup> edition. Oxford: *Blackwell Science, Incorporated*.
- Margalef, R. 1978. Life-forms of phytoplankton as survival alternatives in an unstable environment. *Oceanologica Acta* 1, 493–509.
- Margalef, R. 1979. Functional morphology of organisms involved in red tides, as adapted to decaying turbulence. *Toxic dinoflagellate blooms*, 1:89–94.
- McMinn, A., and Martin, A. (2013). Dark survival in a warming world. *Proceeding of the Royal Society B Biological Science*, 280:20122909.
- Miller, J.H. and S. Moser. 2004. Communication and Coordination. *Complexity*, 9:31-40.
- Peeters, J. C. H., Haas H. A., Peperzak L. and de Vries I., 1993. Nutrients and light as factors controlling phytoplankton biomass on the Dutch Continental Shelf (North Sea) in 1988–1990. Report DGW 93(4). Rijkswaterstaat Tidal Waters division, Middelburg.
- Ras, M., Steyer, J.P., Bernard, O. 2013. Temperature effect on microalgae: a crucial factor for outdoor production. *Reviews in Environmental Science and Biotechnology* 12, 153-164
- Reid, P. C., Edwards, M., Hunt, H.G. and Warner, A.J. 1998. Phytoplankton change in the North Atlantic. *Nature* 391, 546.
- Redfield, A. 1958. The biological control of chemical factors in the environment. *American Scientist* 46, 205–221.
- Reid, P. C., Colebrook, J. M., Matthews, J. B. L., Aiken, J., Barnard, R., Batten, S. D., Beaugrand, G., Buckland, C., Edwards, M., Finlayson, J., Gregory, L., Halliday, N., John, A. W. G., Johns, D., Johnson, A. D., Jonas, T., Lindley, J. A., Nyman, J., Pritchard, P., Richardson, A. J., Saxby, R. E., Sidey, J., Smith, M. A., Stevens, D. P., Tranter, P., Walne, A., Wootton, M., Wotton, C. O. M. & Wright, J. C. 2003. The Continuous Plankton Recorder: concepts and history, from plankton indicator to undulating recorders. *Progress in Oceanography* 58, 117–173.
- Reygondeau, G., and Beaugrand, G. 2010. Water column stability and *Calanus finmarchicus*. *Journal of Plankton Research* 33, 119–136.
- Reynolds, R. W., Rayner, N. A., Smith, T. M., Stokes, D. C., and Wang, W. 2002. An improved *in situ* and satellite SST analysis for climate. *Journal of Climate* 15, 1609–1625.
- Riley, G. A. 1967. The plankton of estuaries. *American Association for the Advancement of Science* 83, 316–326.
- Romagnan, J. B., Legendre, L., Guidi, L., Jamet, J. L., Jamet, D., Mousseau, L., Pedrotti, M. L., Picheral, M., Gorsky, G., Sardet, C., and Stemann, L. 2015. Comprehensive model of annual plankton succession based on the whole-plankton time series approach. *Plos One* 10, e0119219.
- Sathyendranah, S., Ji, R. and Browman, H. I. 2015. Revisiting Sverdrup's critical depth hypothesis. *ICES Journal of Marine Science* 72, 1892–1896.

- Smyth T. J., Allen, I., Atkinson, A., Bruun, J.T., Harmer, R.A., Pingree, R. D., Widdicombe, C. E., and Sommerfield, P. 2014. Ocean net heat flux influences seasonal to interannual patterns of plankton abundance. *Plos One* 9, e98709. DOI:10.1371/journal.pone.0098709.
- Sommer U., Gliwicz, Z., Lampert, W., and Duncan, A. 1986. The Peg-Model of seasonal succession of planktonic events in fresh waters. *Archive of Hydrobiology* 106, 433–471.
- Sommer, U., Adrian, R., De Senerpont Domis, L., Elser, J. J., Gaedke, U., Ibelings, B., Jeppesen, E., Lüring, M., Molinero, J. C., Mooij, W. M., van Donk, E., and Winder, M. 2012. Beyond the Plankton Ecology Group (PEG) model: mechanisms driving plankton succession. *Annual Review of Ecology, Evolution, and Systematics* 43, 429–48.
- Suggett, D. J., Goyen, S., Evenhuis, C., Szabo, M., Pettay, D. T., Warner, M. E. and Ralph, P. J. 2015. Functional diversity of photobiological traits within the genus *Symbiodinium* appears to be governed by the interaction of cell size with cladal designation. *New Phytologist* 208, 370–381.
- Sverdrup, H. U. 1953. On conditions for the vernal blooming of phytoplankton. *Journal du Conseil Permanent International pour l'Exploitation de la Mer* 18, 287–295.
- Ter Braak, C. J. F. 1996. Unimodal models to relate species to environment. Wageningen, DLO-Agricultural Mathematics Group.
- Thackeray, S. J., Henrys, P. A., Hemming, D., Bell, J. R., Botham, M. S., Burthe, S., Helaouët, P., Johns, D. G., Jones, I. D., Leech, D. I., Mackay, E. B., Massimino, D., Atkinson, S., Bacon, P. J., Brereton, T. M., Carvalho, L., Clutton-Brock, T. H., Duck, C., Edwards, M., Elliott, J. M., Hall, S. J. G., Harrington, R., Pearce-Higgins, J. W., Høye, T. T., Kruuk, L. E. B., Pemberton, J. M., Sparks, T. H., Thompson, P. M., White, I., Winfield, I. J., and Wanless, S. 2016. Phenological sensitivity to climate across taxa and trophic levels. *Nature* 535, 241–245.
- Townsend, D. W., Keller, M. D., Sieracki, M. E. & Ackleson, S. G. 1992. Spring phytoplankton blooms in the absence of vertical water column stratification. *Nature* 360, 59–62.
- Tyberghein, L., Verbruggen, H., Pauly, K., Troupin, C., Mineur, F., De Clerck, O. 2012. Bio-ORACLE: A global environmental dataset for marine species distribution modelling. *Global Ecology and Biogeography* 21, 272–81.
- Widdicombe, C. E., Eloire D., Harbour D., Harris, R. P., and Somerfield, P. J. 2010. Long-term phytoplankton community dynamics in the Western English Channel. *Journal of Plankton Research* 32, 643–655.
- Whittaker, R. H. 1975. Communities and ecosystems, 2<sup>nd</sup> edition New York: Macmillan.
- Winder, M., and Cloern, J. E. 2010. The annual cycles of phytoplankton biomass. *Philosophical Transactions of the Royal Society of London B: Biological Sciences* 365, 3215–3226.
- Zhai, L., Platt, T., Tang, C., Sathyendranath, S., and Walne, A. 2013. The response of phytoplankton to climate variability associated with the North Atlantic Oscillation. *Deep Sea Research II Topical Studies in Oceanography* 93, 159–168.

## Figure legends

**Figure 1. Annual changes in the environmental parameters considered in this study.** (a) Sea Surface Temperature (SST), (b) Photosynthetically Active Radiation (PAR), (c) Nitrate, (d) Silicate, (e) and Phosphate concentrations, and (f) Nitrate/Phosphate (N/P) ratio. Note that SST is at a daily resolution whereas other parameters are at a monthly one (see Materials and Methods).

**Figure 2. Annual succession of phytoplankton sorted by PCA.** (a) Species positively and (b) negatively correlated with the first principal component (PC1). (c) Species positively correlated with PC2. (d) Species negatively correlated with PC3. Only annual changes in phytoplankton species with normalised eigenvectors negatively ( $<-0.5$ ) or positively ( $>0.5$ ) correlated to a corresponding principal component were represented. See Table S1 for information on species and their relations to the PCs. Tot. Sp. Richness: total species richness.

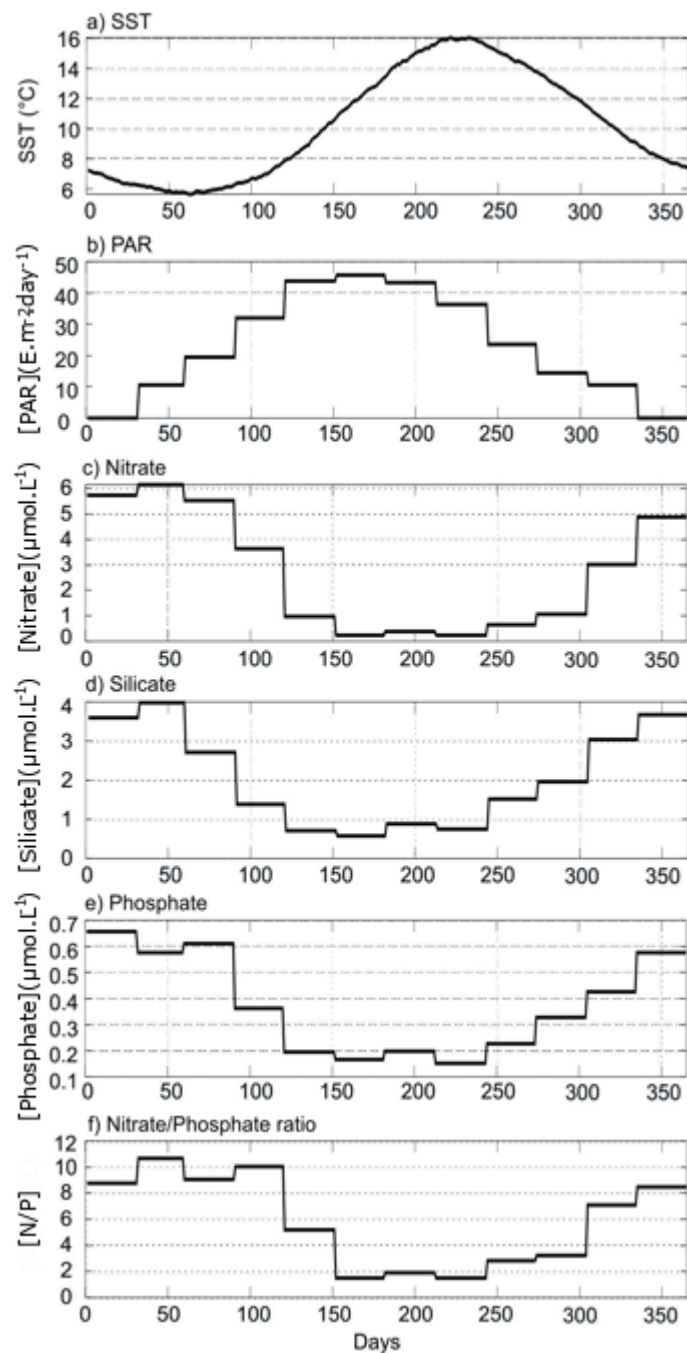
**Figure 3. Reconstructed annual plankton succession from a one-dimensional model based on SST (Sea Surface Temperature, left panels), PAR (Photosynthetically Active Radiation, middle panels) and nitrate (right panels).** A PCA was performed on the relative pseudo-species abundances to identify the most important seasonal phytoplankton abundance patterns. Only predicted plankton seasonal changes, related substantially negatively or positively (i.e., normalised eigenvectors  $>|0.5|$ ) to the Principal Components (PCs) are shown. SST (a-c): species (a) positively and (b) negatively correlated to PC1, (c) species negatively correlated to PC2. SST: Individual pseudo-species abundance is on the left vertical axis. PAR (d-f): species (d) positively and (e) negatively correlated to PC1, (f) species negatively correlated to PC2. Nitrate (g-i): species (g) positively and (h) negatively correlated to PC1, (i) species negatively correlated to PC2. Relative individual pseudo-species abundances generated from METAL are on the left vertical axis.

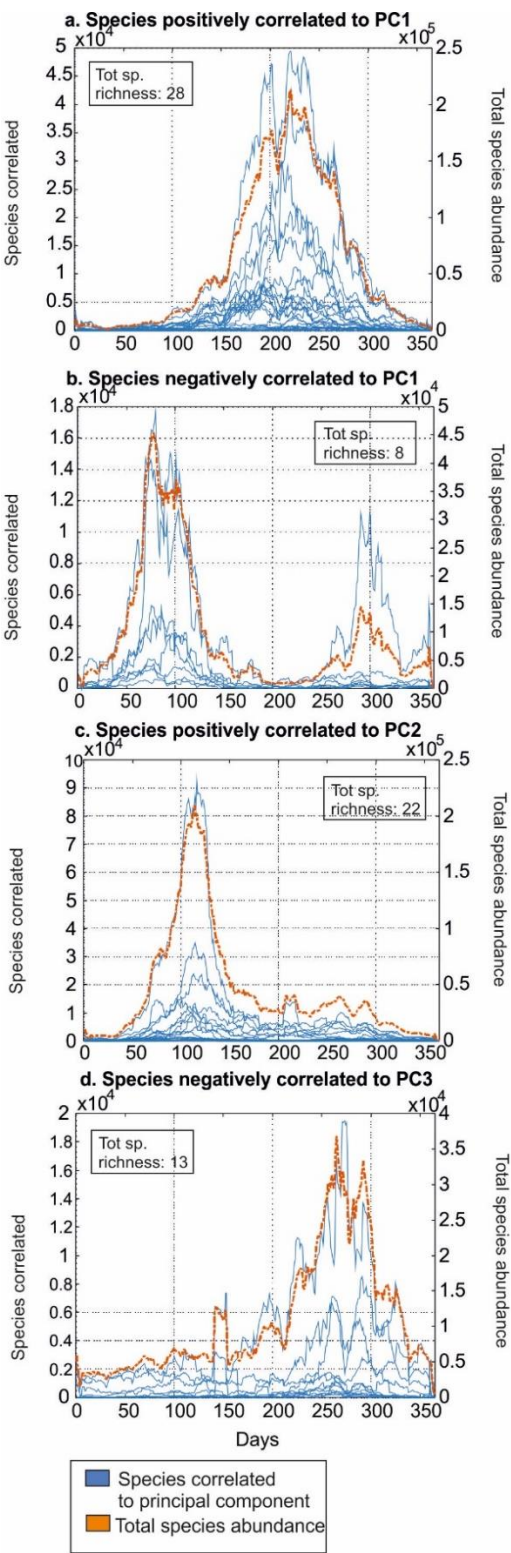
**Figure 4. Reconstructed annual plankton succession from a three-dimensional run based on SST, PAR and nitrate.** A PCA was performed on relative individual pseudo-species abundances to identify the most important seasonal patterns in phytoplankton abundance. Only predicted plankton seasonal changes related substantially negatively or positively (i.e., normalised eigenvectors  $>|0.5|$ ) to the Principal Components (PCs) are shown. Species (a) positively and (b) negatively correlated to PC1. (c) Species negatively correlated to PC2. (d) Species negatively correlated to PC3. (e) Species positively correlated to PC4. Individual pseudo-species abundance is on the left vertical axis.

**Figure 5. Seasonal patterns in standardised observed and simulated phytoplankton species abundances.** Relative abundances of species sampled by the CPR survey (blue) plotted together with relative abundances of pseudo-species reconstructed using METAL (orange). See Table S1 for species names.

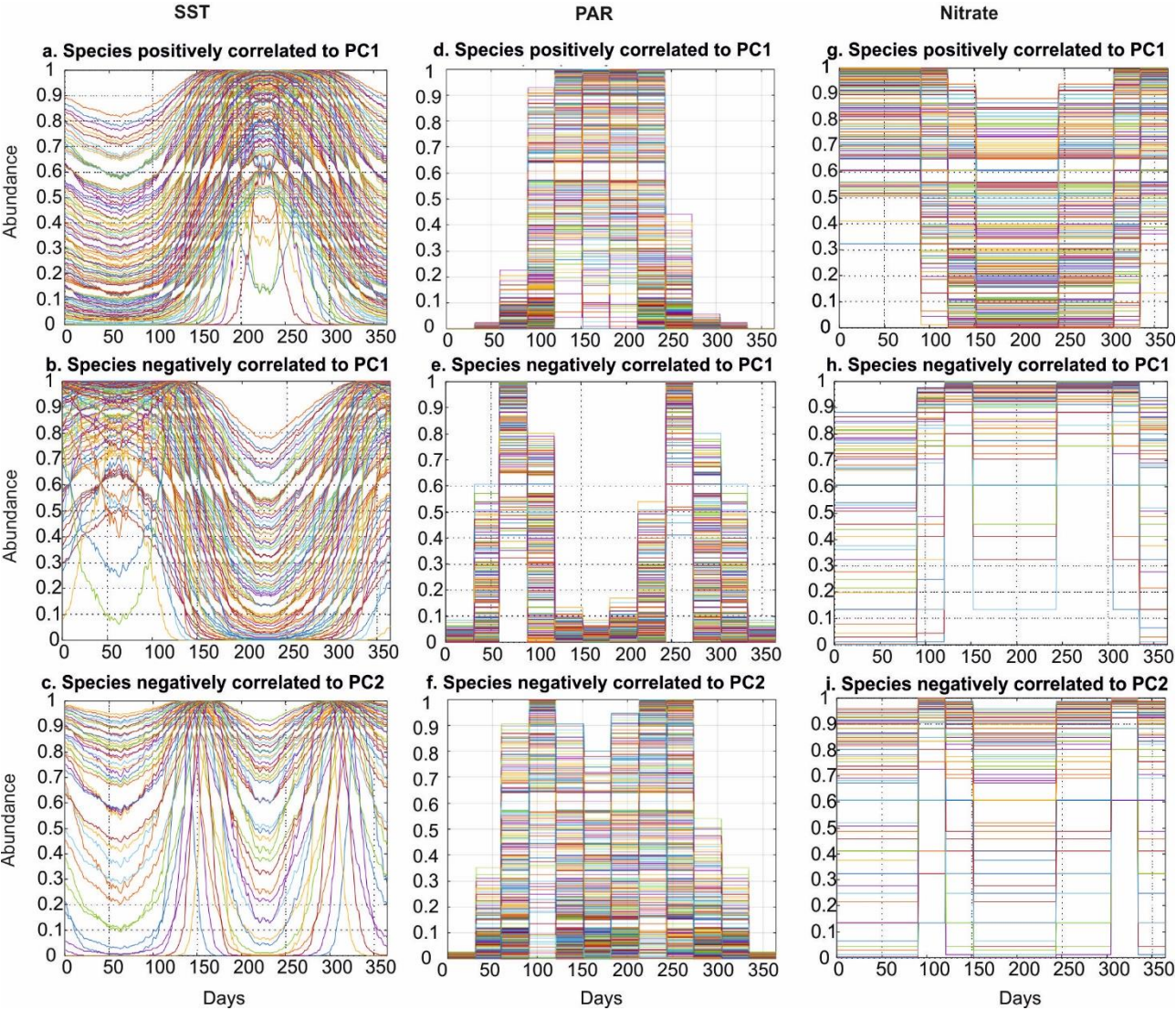
**Figure 6. Identification of the key environmental parameters for reconstructing annual phytoplankton succession.** (a) Number of phytoplankton species exhibiting their highest correlation for each model (run). See Table S2 for the correspondence between run numbers and environmental combinations of variables. (b) Highest correlation for a given phytoplankton species and run. The colorbar shows the linear correlation value.

810 **Figure 1.**





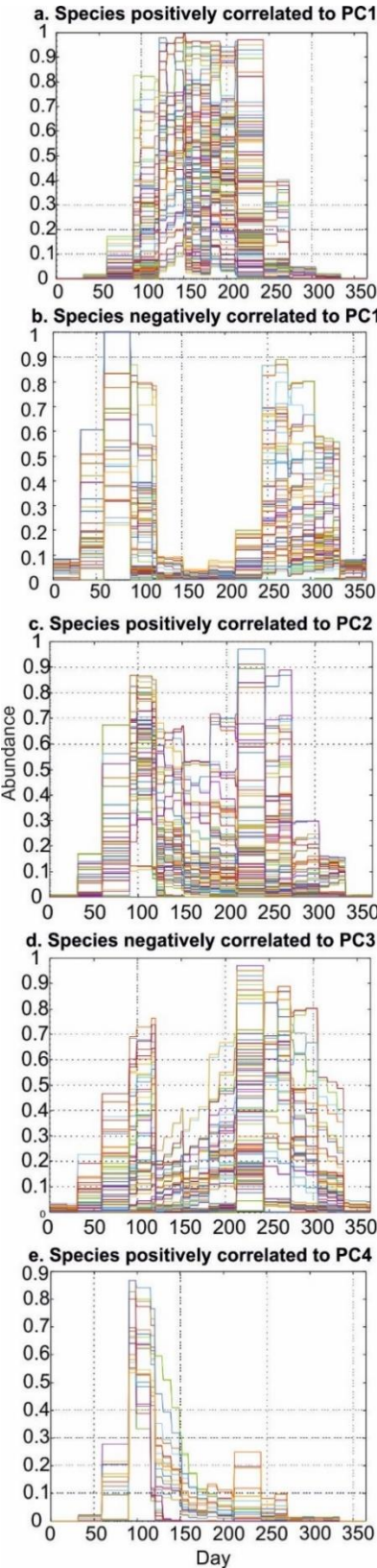




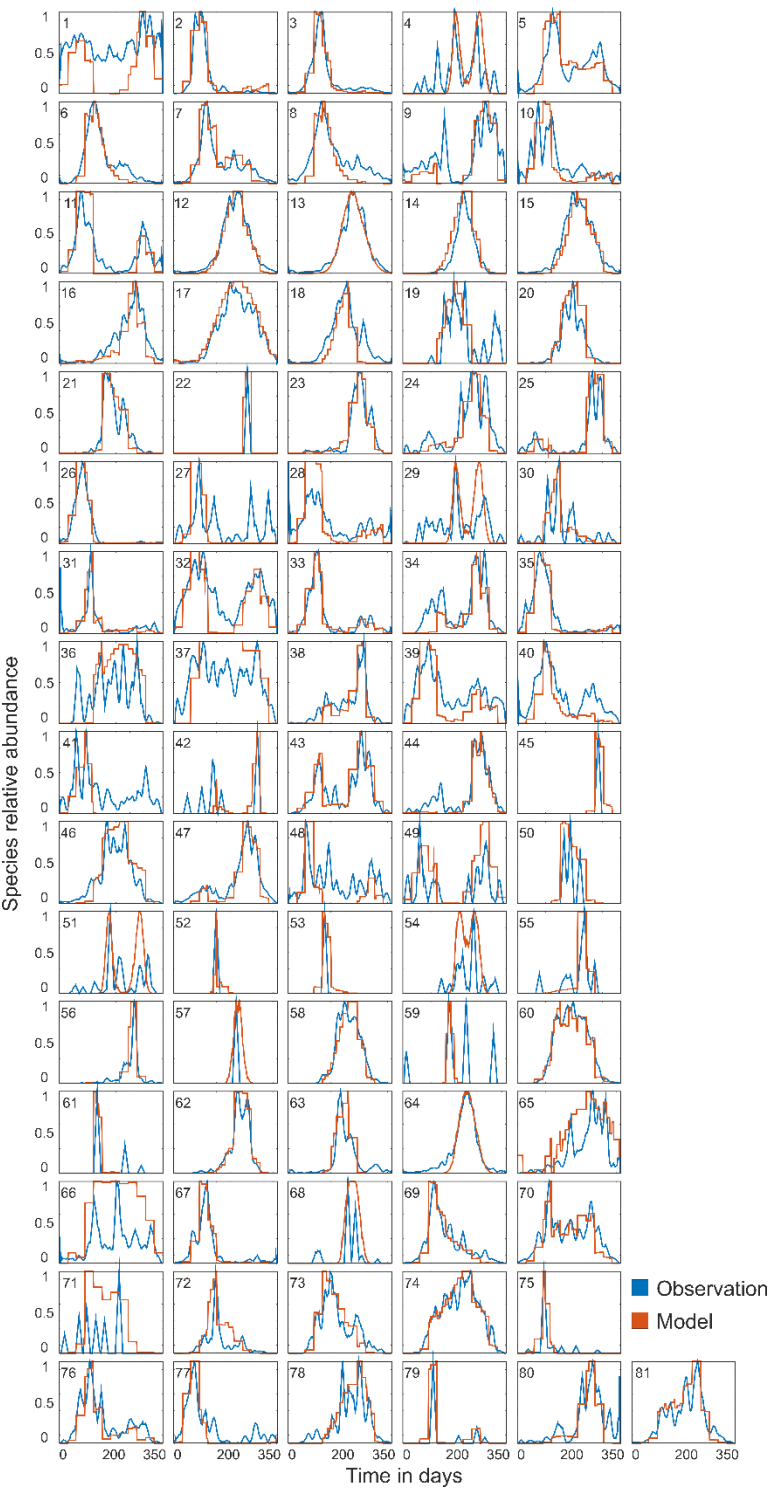
817

818





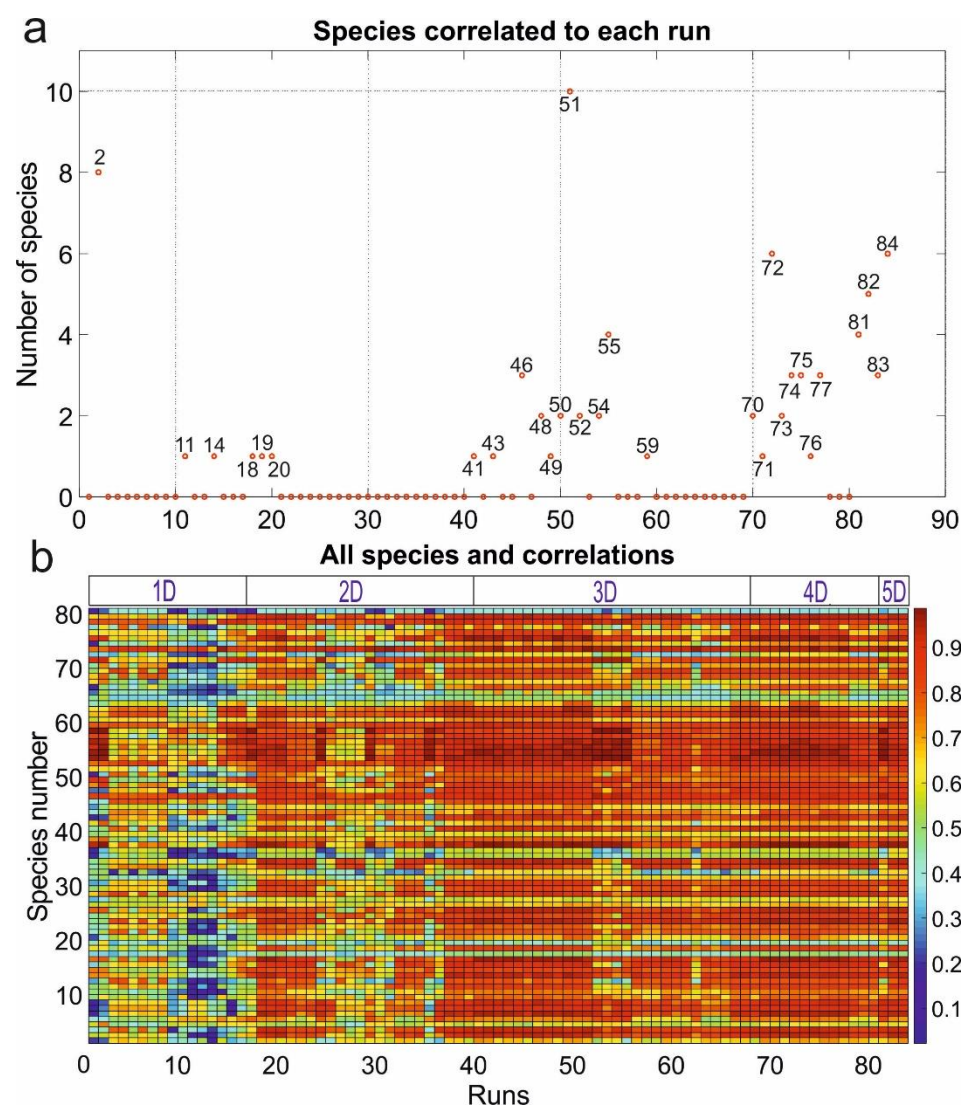
821 **Figure 5.**



822

823

824 **Figure 6.**



## Supporting Information

### Annual phytoplankton succession results from niche-environment interaction

Mariarita Caracciolo<sup>1</sup>, Grégory Beaugrand<sup>2,3,4</sup>, Pierre Helaouët<sup>4</sup>, François Gevaert<sup>3</sup>, Martin Edwards<sup>4,5</sup>, Fabrice Lizon<sup>3</sup>, Loïck Kléparski<sup>2,3,4</sup>, Eric Goberville<sup>6</sup>.

<sup>1</sup>*Sorbonne Université, CNRS, Station Biologique de Roscoff, UMR 7144, ECOMAP, Place Georges Teissier, 29680 Roscoff, France.*

<sup>2</sup>*Centre National de la Recherche Scientifique (CNRS), Université de Lille, Université Littoral Côte d'Opale, UMR 8187 LOG, Laboratoire d'Océanologie et de Géosciences, F 62930 Wimereux, France.*

<sup>3</sup>*Université de Lille, CNRS, Univ. Littoral Côte d'Opale, UMR 8187, LOG, Laboratoire d'Océanologie et de Géosciences, F 62930 Wimereux, France.*

<sup>4</sup>*Marine Biological Association, Continuous Plankton Recorder (CPR) survey, Citadel Hill, Plymouth PL1 2PB, UK.*

<sup>5</sup>*University of Plymouth, School of Biological and Marine Sciences, Drake Circus, Plymouth, UK.*

<sup>6</sup>*Unité Biologie des organismes et écosystèmes aquatiques (BOREA), Muséum National d'Histoire Naturelle, Sorbonne Université, Université de Caen Normandie, Université des Antilles, CNRS, IRD, CP53, 61, Rue Buffon 75005 Paris, France.*

**Corresponding authors:** Mariarita Caracciolo ([mariarita.caracciolo@sb-roscoff.fr](mailto:mariarita.caracciolo@sb-roscoff.fr)) and Gregory Beaugrand ([Gregory.Beaugrand@univ-lille1.fr](mailto:Gregory.Beaugrand@univ-lille1.fr))

## Supplementary Figures and Tables Legends

**Figure S1. Location of the study area.** The geographical boundary of the rectangle (black box) is 54-56°N and 1-4°E.

**Figure S2. Thermal niche (bottom) and the associated theoretical response (top) of a hypothetical species to the fluctuations of an environmental parameter.** The optimal value ( $x_{opt}$ ) of the ecological niche corresponds to the centre of the species' distributional range and is associated with the highest species' abundance that is located in the optimum zone between the two points  $X_s$ . The bimodal distribution of temporal variability exhibits a maximum  $V_{max}$  corresponding to greatest slopes (XHV; HV for High Variability) of the niche.  $X_D$  is the threshold from where environmental fluctuations are unlikely to be detected because the species' ecological sensitivity becomes too small.  $X_L$  are the values where environmental variability becomes lethal. The grey areas indicate the region where the response of the species to environmental changes is expected to be strong. From Beaugrand and Kirby (2016).

**Figure S3. Average correlation (a) and Mean Absolute Error (MAE) (b) for each run used to reconstruct annual phytoplankton succession from uni-dimensional (1D) to 5-dimensional (5D) models.** The average value (blue circle) was based on the best correlations (a) or MAEs (b) assessed between observed species and (simulated) pseudo-species. Black and red points show the results of the same calculations based on a null model with (red) and without (black) consideration of temporal autocorrelation.

**Table S1. List of phytoplankton species and their correlation with the first four principal components (PCs).** List of phytoplankton species considered in our study area (see Fig. S1). The 81 species were grouped in the following classes: 1: Bacillariophyceae, 2: Dinophyceae, 3: Primmnesiophyceae, 4: Dictyochophyceae and 5: Cyanophyceae. The first four PCs considered in Fig. 2 and their eigenvalues are reported here. A cross indicates a significant correlation ( $> |0.5|$ ) between a species and a principal component. Some species were not correlated. The percentage of explained variance per principal component is indicated into brackets. The seasonal cycles of each phytoplankton species are represented on Fig. S4 (see species numbers, first column of this table, for correspondence).

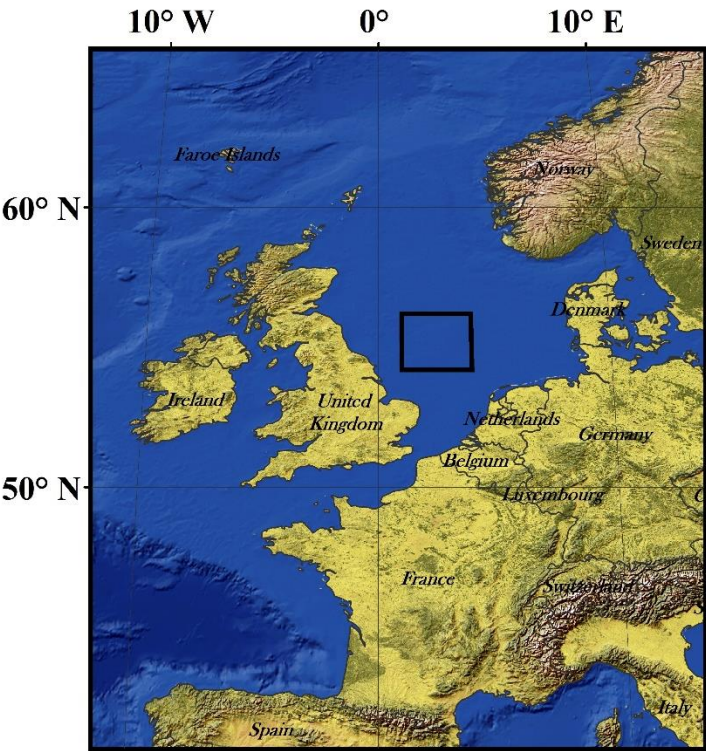
**Table S2. Model simulations.** Information on the 84 runs based on all possible combinations of environmental parameters from one (1D; uni-dimensional) to five (5D; 5-dimensional) variables. T: Sea Surface Temperature, T<sub>his</sub>: Sea Surface Temperature using a higher number of niches, PAR<sub>a,b,c</sub>: Photosynthetically Active Radiation (the letters represent 3 different measures used to calculate the optimum values,  $E.m^{-2}.day^{-1}$ ; see text and Table S3 for details), N: Nitrate ( $\mu mol.L^{-1}$ ), S: Silicate ( $\mu mol.L^{-1}$ ), P: Phosphate ( $\mu mol.L^{-1}$ ), N/P: Nitrate/Phosphate ratio (see Table S3 for a better understanding of the selected SST and PAR values). For each run, computation time required for building pseudo-species and calculating species abundances is reported.

**Table S3. Environmental variables used for the calculation of pseudo-species abundances and respective optimum and tolerance values.** For each environmental parameter the table shows the different range of optimum values and ecological amplitudes defined for niche construction. We used several resolutions (first column) to calculate the environmental niche. For runs ended by "bis", the resolution was improved to examine model sensitivity related to the number of points used to calculate the niche. To examine the sensitivity of our analysis to PAR,

three categories (a, b, c) were determined by selecting different minimum values (see text). When more than one factor was considered, the number of niches was multiplied by each ecological dimension to obtain the total number of niches (see text).

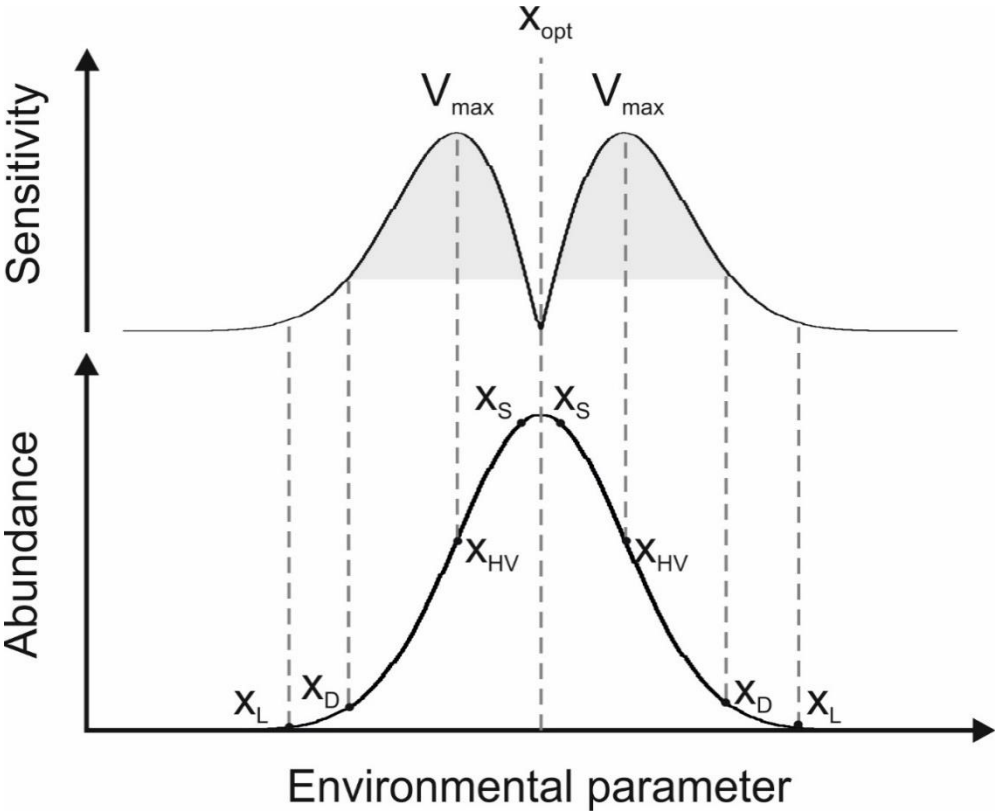
**Table S4. Statistics calculated for the different runs, using several combinations of environmental parameters.** For each combination of environmental parameters, the number of species, mean and maximum correlation values and probability values that result from the application of null models for both the Pearson correlation and MAE, with and without consideration of temporal autocorrelation, are reported.

920    **Figure S1.**

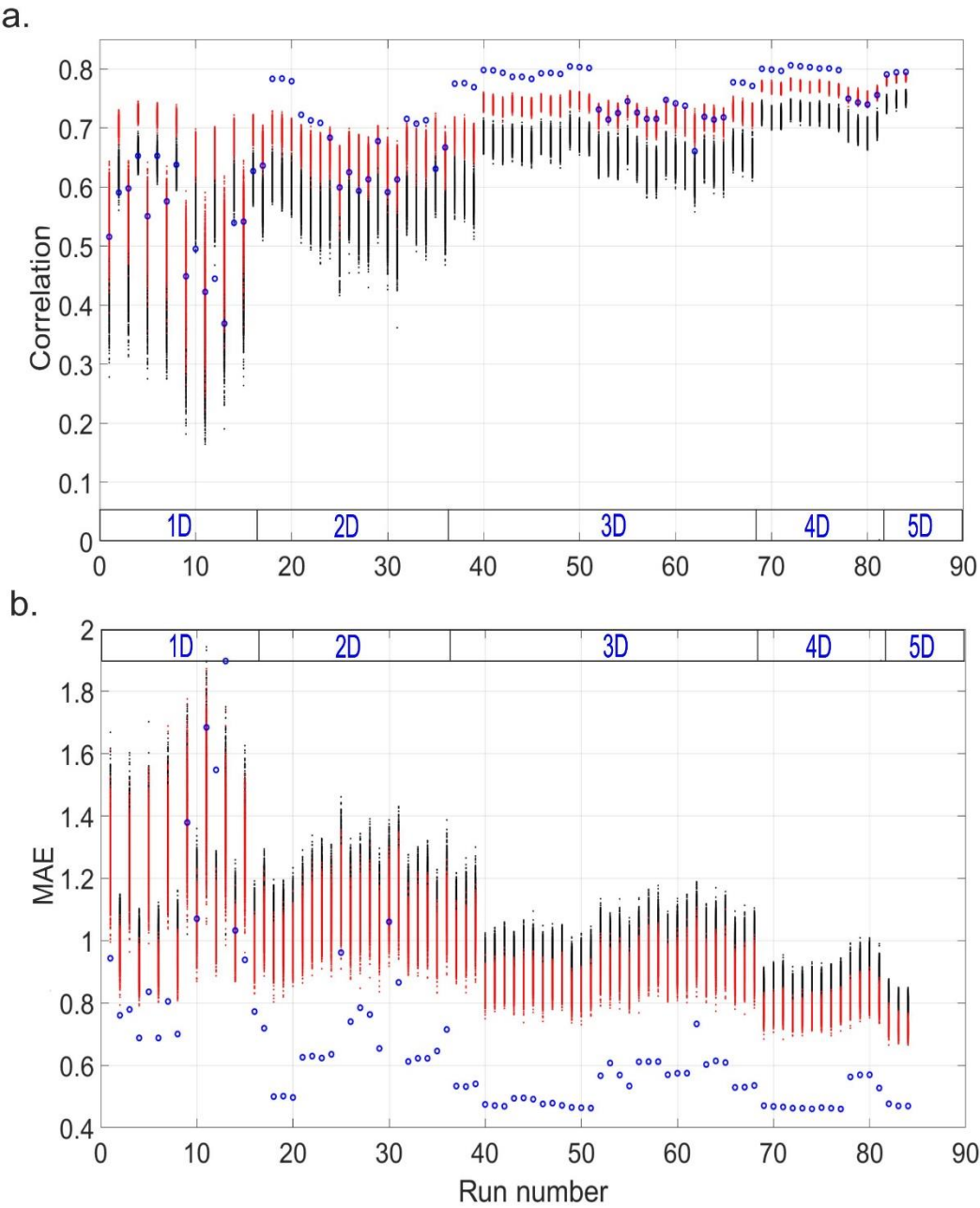


921

922







Category	Phytoplankton species	PC1 (26.86 %)	PC2 (18.06 %)	PC3 (12.22 %)	PC4 (5.45 %)
<b>Phylum: Ochrophyta</b>					
<b>Class: Bacillariophyceae</b>					
1	<i>Paralia sulcata</i>			X	
2	<i>Skeletonema costatum</i>	X	X		
3	<i>Thalassiosira</i> spp.		X		
4	<i>Dactylosolen antarcticus</i>	X			
5	<i>Rhizosolenia styliformis</i>		X		
6	<i>Rhizosolenia hebetata semispina</i>		X		
7	<i>Chaetoceros</i> (Hyalochaete) spp.		X		
8	<i>Chaetoceros</i> (Phaeoceros) spp.		X		
9	<i>Odontella sinensis</i>			X	
10	<i>Thalassiothrix longissima</i>		X		
11	<i>Thalassionema nitzschioides</i>	X			
22	<i>Asteromphalus</i> spp.				
23	<i>Bacteriastrium</i> spp.	X		X	
24	<i>Bellerochea malleus</i>	X		X	
25	<i>Biddulphia alternans</i>			X	
26	<i>Odontella aurita</i>	X			X
27	<i>Odontella granulata</i>				
28	<i>Odontella regia</i>	X	X		
29	<i>Odontella rhombus</i>				
30	<i>Cerataulina pelagica</i>				X
31	<i>Coscinodiscus concinnus</i>		X		
32	<i>Coscinodiscus</i> spp. (Unidentified)	X	X		
33	<i>Ditylum brightwellii</i>	X	X		
34	<i>Eucampia zodiacus</i>		X	X	
35	<i>Fragilaria</i> spp.	X			
36	<i>Guinardia flaccida</i>				
37	<i>Gyrosigma</i> spp.		X		
38	<i>Leptocylindrus danicus</i>	X			
39	<i>Navicula</i> spp.		X		
40	<i>Cylindrotheca closterium</i>		X		
41	<i>Rhaphoneis amphiceros</i>				
42	<i>Rhizosolenia bergonii</i>				
43	<i>Rhizosolenia setigera</i>		X		
44	<i>Stephanopyxis</i> spp.			X	
48	<i>Nitzschia</i> spp. (Unidentified)				
49	<i>Odontella mobilensis</i>			X	
64	<i>Proboscía alata</i>	X			
65	<i>Leptocylindrus mediterraneus</i>	X		X	
66	<i>Proboscía inermis</i>				
67	<i>Asterionellopsis glacialis</i>		X		
68	<i>Ephemera planamembranacea</i>				
69	<i>Pseudo-nitzschia delicatissima</i> complex		X		
70	<i>Pseudo-nitzschia seriata</i> complex		X		
72	<i>Guinardia delicatula</i>				X
73	<i>Dactylosolen fragilissimus</i>		X		
74	<i>Guinardia striata</i>	X			
76	<i>Lauderia annulata</i>		X		
77	<i>Bacillaria paxillifera</i>	X			
78	<i>Corethron hystris</i>	X			
79	<i>Proboscía curvirostris</i>		X		
80	<i>Proboscía indica</i>	X		X	
81	<i>Rhizosolenia imbricata</i>	X			
75	<i>Helicotheca tamesis</i>				
<b>Class: Dictyochophyceae</b>					
47	<i>Silicoflagellates</i>	X		X	
<b>Phylum: Dinoflagellata</b>					
<b>Class: Dinophyceae</b>					
12	<i>Ceratium fusus</i>	X			
13	<i>Ceratium furca</i>	X			
14	<i>Ceratium lineatum</i>	X			
15	<i>Ceratium tripos</i>	X			
16	<i>Ceratium macroceras</i>	X		X	
17	<i>Ceratium horridum</i>	X			
18	<i>Ceratium longipes</i>	X			
19	<i>Ceratium arcticum</i>	X			
20	<i>Dinoflagellate</i> cysts (Total)	X		X	
21	<i>Polykrikos schwartzii</i> cysts	X			
50	<i>Ceratium arietinum</i>				
51	<i>Ceratium bucephalum</i>				
52	<i>Ceratium buceros</i>				X
53	<i>Ceratium carriense</i>				
54	<i>Ceratium hexacanthum</i>	X			
55	<i>Ceratium massiliense</i>	X			
56	<i>Ceratium minutum</i>			X	
57	<i>Ceratium teres</i>				
58	<i>Dinophysis</i> spp. Total	X			
59	<i>Oxytoxum</i> spp.				
60	<i>Protoperidinium</i> spp.	X			
61	<i>Pronoctiluca pelagica</i>				
62	<i>Prorocentrum</i> spp. Total	X			
63	<i>Noctiluca scintillans</i>	X			
<b>Phylum: Haptophyta</b>					
<b>Class: Prymnesiophyceae</b>					
45	<i>Phaeocystis pouchetii</i>				
46	<i>Coccolithaceae</i> (Total)	X			
<b>Phylum: Cyanobacteria</b>					
<b>Class: Cyanophyceae</b>					
71	<i>Trichodesmium</i> spp.				

Run n°	Dimension	Variable	Computation time (hh:mm:ss)
Run 1	1D	T	00:00:05
Run 2	1D	T bis	00:00:08
Run 3	1D	PARa	00:00:13
Run 4	1D	PARa bis	00:00:17
Run 5	1D	PARb	00:00:21
Run 6	1D	PARb bis	00:00:25
Run 7	1D	PARc	00:00:05
Run 8	1D	PARc bis	00:00:08
Run 9	1D	N	00:00:05
Run 10	1D	N bis	00:00:08
Run 11	1D	S	00:00:05
Run 12	1D	S bis	00:00:08
Run 13	1D	P	00:00:05
Run 14	1D	P bis	00:00:08
Run 15	1D	N/P	00:00:05
Run 16	1D	N/P bis	00:00:08
Run 17	2D	T and N	00:02:00
Run 18	2D	T and PARa	00:05:00
Run 19	2D	T and PARb	00:03:30
Run 20	2D	T and PARc	00:02:00
Run 21	2D	N and PARa	00:05:00
Run 22	2D	N and PARb	00:03:30
Run 23	2D	N and PARc	00:02:00
Run 24	2D	T and S	00:02:00
Run 25	2D	N and S	00:02:00
Run 26	2D	S and PARa	00:05:00
Run 27	2D	S and PARb	00:03:30
Run 28	2D	S and PARc	00:02:00
Run 29	2D	T and P	00:02:00
Run 30	2D	N and P	00:02:00
Run 31	2D	S and P	00:02:00
Run 32	2D	P and PARa	00:05:00
Run 33	2D	P and PARb	00:03:30
Run 34	2D	P and PARc	00:02:00
Run 35	2D	T and N/P	00:02:00
Run 36	2D	S and N/P	00:02:00
Run 37	2D	N/P and PARa	00:05:00
Run 38	2D	N/P and PARb	00:18:00
Run 39	2D	N/P and PARc	00:15:00
Run 40	3D	T,N and PARa	00:20:00
Run 41	3D	T,N and PARb	00:18:00
Run 42	3D	T,N and PARc	00:15:00
Run 43	3D	T,S and PARa	00:20:00
Run 44	3D	T,S and PARb	00:18:00
Run 45	3D	T,S and PARc	00:15:00
Run 46	3D	T,P and PARa	00:20:00
Run 47	3D	T,P and PARb	00:18:00
Run 48	3D	T,P and PARc	00:15:00
Run 49	3D	T,N/P and PARa	00:20:00
Run 50	3D	T,N/P and PARb	00:18:00
Run 51	3D	T,N/P and PARc	00:15:00
Run 52	3D	T,N and S	00:15:00
Run 53	3D	T,N and P	00:15:00
Run 54	3D	T,S and P	00:15:00
Run 55	3D	T,S and NP	00:15:00
Run 56	3D	N,S and PARa	00:20:00
Run 57	3D	N,S and PARb	00:18:00
Run 58	3D	N,S and PARc	00:15:00
Run 59	3D	N,P and PARa	00:20:00
Run 60	3D	N,P and PARb	00:18:00
Run 61	3D	N,P and PARc	00:15:00
Run 62	3D	N,S and P	00:15:00
Run 63	3D	S,P and PARa	00:20:00
Run 64	3D	S,P and PARb	00:18:00
Run 65	3D	S,P and PARc	00:15:00
Run 66	3D	S,N/P and PARa	00:20:00
Run 67	3D	S,N/P and PARb	00:18:00
Run 68	3D	S,N/P and PARc	00:15:00
Run 69	4D	T, N, S, PARa	96:00:00
Run 70	4D	T, N, S, PARb	72:00:00
Run 71	4D	T, N, S, PARc	60:00:00
Run 72	4D	T, N/P, PARa,S	120:00:00
Run 73	4D	T, N/P, PARb,S	96:00:00
Run 74	4D	T, N/P, PARc,S	72:00:00
Run 75	4D	T, N, P, PARa	36:00:00
Run 76	4D	T, N, P, PARb	36:00:00
Run 77	4D	T, N, P, PARc	24:00:00
Run 78	4D	S, N,P,PARa	60:00:00
Run 79	4D	S, N,P,PARb	60:00:00
Run 80	4D	S, N,P,PARc	48:00:00
Run 81	4D	T, N, S, P	48:00:00
Run 82	5D	T, N, S, P, PARc	480:00:00
Run 83	5D	T,N,S,P,PARb	984:00:00
Run 84	5D	T,N,S,P,PARa	1176:00:00



933 **Table S3.**

Environmental variable	Optimum	Number of optimum values	Tolerance	Number of ecological amplitudes	Number of niches
Temperature= -2,-1,0,...,44	0,6,12,...,36	7	1,4,7,10	4	28
Temperature bis= -2,1.99,1.98,...,44	0,1,2,...,40	41	1,2,3,...,40	10	410
PARa= 0,1,2,...,70	1,9,17,...,70	9	1,5,9	3	27
PARa bis= 0,0.25,0.50,...,70	1,2,3,...,70	70	1,2,3,...,9	9	630
PARb= 0,1,2,...,70	10,18,26,...,70	8	1,5,9	3	24
PARb bis= 0,0.25,0.50,...,70	10,11,12,...,70	60	1,2,3,...,9	9	540
PARc= 0,1,2,...,70	20,28,36,...,70	7	1,5,9	3	21
PARc bis= 0,0.25,0.50,...,70	20,21,22,...,70	50	1,2,3,...,9	9	450
Nitrate= 0,1,2,...,43	1,6,11,...,41	9	1,4,7	3	27
Nitrate bis= 0,0.01,0.02,...,43	1,2,3,...,41	41	1,2,3,...,7	7	287
Silicate= 0,1,2,...,127	1,20,39,...,126	7	1,6,11,16	4	28
Silicate bis= 0,0.1,0.2,...,127	1,4,7,...,126	42	1,2,3,...,16	16	672
Phosphate= 0,0.1,0.2,...,3.8	0.1,0.4,3.5	3	0.1,0.3,0.5	3	27
Phosphate bis= 0,0.01,0.02,...,3.8	0.1,0.2,0.3,...,3.5	35	0.1,0.13,0.16,...,0.5	16	560
N/P= 0,0.2,0.4,...,25	0,4,8,...,24	7	1,2,3,4	4	28
N/P bis= 0,0.01,0.02,...,25	0,1,2,...,24	25	1,1.25,1.50,...,4	16	400

934

935

936

		Phytoplankton			Null model	Null model	Null model	Null model
					Correlation	Correlation	MAE	MAE
					Without autocorrelation	With autocorrelation	Without autocorrelation	With autocorrelation
Run n°	Parameters	Mean correlation	Species correlated	Highest correlations	Probability	Probability	Probability	Probability
Run 1	T	0,5156	0	-	2,8	83,8	0	0
Run 2	T.bis	0,5906	8	0,7676	98,3	100	0	0
Run 3	PARa	0,5976	0	-	0	15,7	0	0
Run 4	PARa.bis	0,6527	0	-	59,4	100	0	0
Run 5	PARb	0,5506	0	-	0,1	49,3	0	0
Run 6	PARb.bis	0,6527	0	-	33,9	100	0	0
Run 7	PARc	0,5757	0	-	0	12,3	0	0
Run 8	PARc.bis	0,6376	0	-	42,9	100	0	0
Run 9	N	0,4488	0	-	3,1	66,6	24,5	46,5
Run 10	N.bis	0,4951	0	-	99,7	100	5,4	55,8
Run 11	S	0,4224	1	0,6937	3,9	52	88,4	94,7
Run 12	S.bis	0,4447	0	-	100	100	100	100
Run 13	P	0,3687	0	-	61,3	99	100	100
Run 14	P.bis	0,5392	1	0,6318	99,8	100	7,6	77,5
Run 15	N/P	0,5414	0	-	0,2	62,1	0	0
Run 16	N/P.bis	0,6270	0	-	25,7	100	0	0
Run 17	T and N	0,6362	0	-	0,1	98,8	0	0
Run 18	T and PARa	0,7833	1	0,8790	0	0	0	0
Run 19	T and PARb	0,7838	1	0,8344	0	0	0	0
Run 20	T and PARc	0,7791	1	0,7589	0	0	0	0
Run 21	N and PARa	0,7224	0	-	0	0	0	0
Run 22	N and PARb	0,7128	0	-	0	0	0	0
Run 23	N and PARc	0,7085	0	-	0	0	0	0
Run 24	T and S	0,6835	0	-	0	3,9	0	0
Run 25	N and S	0,5993	0	-	0,1	77,7	0	0,7
Run 26	S and PARa	0,6251	0	-	0,2	98,6	0	0
Run 27	S and PARb	0,5933	0	-	3,2	99,9	0	0
Run 28	S and PARc	0,6129	0	-	0,2	93,1	0	0
Run 29	T and P	0,6776	0	-	0	28,9	0	0
Run 30	N and P	0,5912	0	-	0,9	98,5	1,5	19,1
Run 31	S and P	0,6127	0	-	0,1	66,7	0	0
Run 32	P and PARa	0,7153	0	-	0	0	0	0
Run 33	P and PARb	0,7073	0	-	0	0,1	0	0
Run 34	P and PARc	0,7130	0	-	0	0	0	0
Run 35	T and N/P	0,6308	0	-	8,4	100	0	0
Run 36	S and N/P	0,6670	0	-	0	17,4	0	0
Run 37	N/P and PARa	0,7751	0	-	0	0	0	0
Run 38	N/P and PARb	0,7759	0	-	0	0	0	0
Run 39	N/P and PARc	0,7690	0	-	0	0	0	0
Run 40	T,N and PARa	0,7981	0	-	0	0	0	0
Run 41	T,N and PARb	0,7975	1	0,8276	0	0	0	0
Run 42	T,N and PARc	0,7934	0	-	0	0	0	0
Run 43	T,S and PARa	0,7866	1	0,9613	0	0	0	0
Run 44	T,S and PARb	0,7866	0	-	0	0	0	0
Run 45	T,S and PARc	0,7831	0	-	0	0	0	0
Run 46	T,P and PARa	0,7925	3	0,9384	0	0	0	0
Run 47	T,P and PARb	0,7931	0	-	0	0	0	0
Run 48	T,P and PARc	0,7915	2	0,9162	0	0	0	0
Run 49	T,N/P and PARa	0,8043	1	0,8913	0	0	0	0
Run 50	T,N/P and PARb	0,8031	2	0,7807	0	0	0	0
Run 51	T,N/P and PARc	0,8016	10	0,8644	0	0	0	0
Run 52	T,N and S	0,7313	2	0,8896	0	7,9	0	0
Run 53	T,N and P	0,7142	0	-	0	97,8	0	0
Run 54	T,S and P	0,7253	2	0,9691	0	34,2	0	0
Run 55	T,S and NP	0,7452	4	0,8548	0	4,7	0	0
Run 56	N,S and PARa	0,7261	0	-	0	24,3	0	0
Run 57	N,S and PARb	0,7154	0	-	0	19,6	0	0
Run 58	N,S and PARc	0,7154	0	-	0	21,5	0	0
Run 59	N,P and PARa	0,7475	1	0,4239	0	0,1	0	0
Run 60	N,P and PARb	0,7415	0	-	0	0,1	0	0
Run 61	N,P and PARc	0,7374	0	-	0	0	0	0
Run 62	N,S and P	0,6605	0	-	0,1	100	0	0
Run 63	S,P and PARa	0,7189	0	-	0	53,8	0	0
Run 64	S,P and PARb	0,7141	0	-	0	53,4	0	0
Run 65	S,P and PARc	0,7180	0	-	0	14,8	0	0
Run 66	S,N/P and PARa	0,7774	0	-	0	0	0	0
Run 67	S,N/P and PARb	0,7767	0	-	0	0	0	0
Run 68	S,N/P and PARc	0,7710	0	-	0	0	0	0
Run 69	T, N, S, PARa	0,8002	0	-	0	0	0	0
Run 70	T, N, S, PARb	0,7988	2	0,8240	0	0	0	0
Run 71	T, N, S, PARc	0,7966	1	0,9490	0	0	0	0
Run 72	T, NP, PARa,S	0,8062	6	0,8390	0	0	0	0
Run 73	T, NP, PARb,S	0,8045	2	0,8274	0	0	0	0
Run 74	T, NP, PARc,S	0,8030	3	0,7431	0	0	0	0
Run 75	T, N, P, PARa	0,8008	3	0,8920	0	0	0	0
Run 76	T, N, P, PARb	0,8008	1	0,7896	0	0	0	0
Run 77	T, N, P, PARc	0,7980	3	0,8575	0	0	0	0
Run 78	S, N,P,PARa	0,7497	0	-	0	90,8	0	0
Run 79	S, N,P,PARb	0,7431	0	-	0	96	0	0
Run 80	S, N,P,PARc	0,7397	0	-	0	97,1	0	0
Run 81	T, N, S, P	0,7558	4	0,8849	0	76,5	0	0
Run 82	T, N, S, P,PARc	0,7906	5	0,7922	0	0	0	0
Run 83	T,N,S,P,PARb	0,7941	3	0,8741	0	0	0	0
Run 84	T,N,S,P,PARa	0,7948	6	0,8378	0	0	0	0